



**CFD analysis of
thermal energy harvesting from heat sources.**

By

Waleed Ahmad

Master Thesis Submitted to
ICAI School of Engineering - Universidad Pontificia Comillas
In the fulfillment of the Requirements
For Master's Degree in Sapienza University of Rome

Director:

Borja Rengel Darnaculleta

Declaro, bajo mi responsabilidad, que el Proyecto presentado con el título
CFD analysis of thermal energy harvesting from heat sources
en la ETS de Ingeniería - ICAI de la Universidad Pontificia Comillas en el
curso académico 2022//2023 es de mi autoría, original e inédito y
no ha sido presentado con anterioridad a otros efectos. El Proyecto no es
plagio de otro, ni total ni parcialmente y la información que ha sido tomada

Fdo.: Waleed AHMAD

Fecha: 13/07/2023



Autorizada la entrega del proyecto

Fdo.: Borja RENGEL

Fecha: 13/07/2023



Abstract

The thermoelectric energy harvesting technology describes the conversion of temperature gradient into electric power via thermoelectric generator (TEG) device. Although this device is mainly aimed at generating electricity in applications in which heat would be otherwise dissipated, intentionally heat sources could be originated to produce power.

By having waste incineration process in many regions of world, energy is being wasted to the environment. The main objective of this study is to assess the power from different types of waste incineration. After a detailed review of the study papers regarding waste production, management, and handling helped us to choose the three apt types of waste mentioned below. As the human-controlled fires from debris and waste are leading to a significant temperature increase on the TEG surface, which in turn, lead to a significant power generation by using the CFD (computational fluid dynamics) code Fire Dynamics Simulator (FDS).

This study compares the results of three types of waste wood pellets, rubber and trash cans, and cardboard boxes combustion in different scenarios. Among them the wood pellets combustion with heatsink and lateral wind scenario leads to generate more power.

Acknowledgement

It is a great honour for being an Erasmus student at ICAI School of Engineering-Universidad Pontificia Comillas which provide me the opportunity to accomplish out master's thesis under the kind supervision of Borja Rengel Darnacullea. He always has been a source of motivation and encouragement through his valuable feedback, expert suggestions, and friendly behaviour throughout the process of writing of this thesis. I also want to pay my special thanks to Paolo Venturini, supervisor from my home University, Sapienza University of Rome who accepted this thesis proposal to be completed during my exchange program period. Lastly, I am so much obliged to all my friends who helped and encouraged me to complete this task.

Contents

Abstract	i
Acknowledgement.....	ii
Chapter 1	1
Introduction	1
1.1 Introduction	1
1.2 Background	1
1.3 Study motivation	1
1.4 Objective of study	2
Chapter 2	3
Literature Review	3
2.1 Thermoelectric Generators (TEGs).....	3
2.1.1 About TEG	3
2.1.2 Materials used to design the TEG.	5
2.1.3 Mathematical modelling of TEG.....	6
2.1.4 Cooling systems of TEG	8
2.1.5 Applications of TEGs.....	10
2.2 Potential heat sources from wastes and biomass.....	11
2.2.1 Waste generation worldwide	11
2.2.2 Waste materials	12
2.2.3 Waste management	12
2.2.4 Heating values of waste.....	14
2.2.5 Emissions from waste combustion.....	15
2.2.6 Emission control methods	15
Chapter 03.....	18
Methodology	18
3.1 Data collection.....	18
3.1.1 Combustion of the wood pallet and paper.....	19
3.1.2 Combustion of rubber trash can	21
3.1.3 Combustion of cardboard boxes filled with polystyrene cups waste.	23
3.2 CFD analysis	25
3.2.1 Computational Fluid Dynamic (CFD) models	26
3.2.2 Assumptions for FDS (Fire Dynamics Simulator) simulation	27
3.2.3 Dimensions and properties of material for TEG.	28
3.2.4 TEGs' arrangements on CFD model.....	29
3.2.5 Output Power Calculation of TEGs.....	30

Chapter 04	31
Results and Conclusion	31
4.1 FDS Results.....	31
4.1.1 Heat release rate	31
4.1.2 Total heat transfer.....	32
4.1.3 Temperature across the TEGs	32
4.2 Power Generation from TEGs.....	34
4.2.1 Generated Power from wood pellets fire Scenarios	34
4.2.2 Generated Power from rubber and trash can fire Scenarios.....	40
4.2.3 Generated Power from cardboard boxes fire.....	45
4.3 Conclusion.....	51
References	53

List of figures

Figure 1. Schematic of a TEG device with a single thermoelectric couple and two legs [11].....	4
Figure 2. Different designs of TEG, a) lateral type; b) vertical type; c) mixed type.....	5
Figure 3. characteristics of output power curve of thermoelectric generator [18].	7
Figure 4. (a) top-mounted fan (TMF) and (b) side-mounted fan (SMF).....	9
Figure 5. Diagrams illustrating rectangular and round pin heat sink [22].....	9
Figure 6. Schematic diagram of the TEG model and fluid cooling structure.....	10
Figure 7. waste generation, by region (millions of tons/year) [26]	11
Figure 8. Global waste composition (percent) [26].....	12
Figure 9. global waste treatment method	13
Figure 10. Solid waste treatment methods in Spain [30]	14
Figure 11 combustion test process of wood pellets and paper sample.....	20
Figure 12. combustion test process of rubber trash can sample.	22
Figure 13. combustion test process of cardboard boxes sample.	24
Figure 14 The slice file of heat release rate from waste combustion obtained from CFD.	29
Figure 15. radiative heat distribution in boundaries.....	29

List of Graph

Graph 1. heat release rate from wood pellets combustion.	20
Graph 2. heat release rate from rubber and trash can combustion.	22
Graph 3. heat release rate from cardboard boxes combustion.....	24
Graph 4. CFD simulation result, heat release rate of combustion.....	31

Graph 5.CFD simulation result, total heat transfer from combustion.	32
Graph 6. the temperature at front side of TEG 01.....	33
Graph 7. the temperature at colder side of TEG 01.....	33
Graph 8. the generated output power of TEGs and heat release rate from wood pellets waste combustion without heatsink and with no lateral wind.	35
Graph 9. total generated output power of TEGs with wood pellets waste combustion.	35
Graph 10. the generated output power of TEGs and heat release rate from wood pellets waste combustion without heatsink and with lateral wind.	36
Graph 11. total generated output power of TEGs with wood pellets waste combustion without heatsink and with lateral wind.....	37
Graph 12. the generated output power of TEGs and heat release rate from wood pellets waste combustion with heatsink and with no lateral wind.	37
Graph 13. total generated output power of TEGs with wood pellets waste combustion.	38
Graph 14. the generated output power of TEGs and heat release rate from wood pellets waste combustion with heatsink and with lateral wind.....	39
Graph 15. total generated output power of TEGs with wood pellets waste combustion.	39
Graph 16.generated output power of TEGs and heat release rate from rubber and trash can waste combustion without heatsink and with no lateral wind.	40
Graph 17. total generated output power of TEGs with rubber and trash cans waste combustion without heatsink and with no lateral wind.....	41
Graph 18. generated output power of TEGs and heat release rate from rubber and trash can waste combustion without heatsink and with lateral wind.....	41
Graph 19. total generated output power of TEGs with rubber and trash cans waste combustion without heatsink and with lateral wind.	42
Graph 20. generated output power of and with heat release rate from rubber and trash can waste combustion with heatsink and without lateral wind.....	43
Graph 21. total generated output power of TEGs with rubber and trash cans waste combustion with heatsink and with no lateral wind.....	43
Graph 22. generated output power of TEGs and with heat release rate from rubber and trash can waste combustion with heatsink and with lateral wind.	44
Graph 23. total generated output power of TEGs with rubber and trash cans waste combustion with heatsink and with lateral wind.....	45
Graph 24. generated output power of TEGs and heat release rate from cardboard boxes waste combustion without heatsink and with no lateral wind.	46
Graph 25. total generated output power of TEGs with cardboard boxes waste combustion.....	46
Graph 26. generated output power of TEGs and heat release rate from cardboard boxes waste combustion without heatsink and with lateral wind.	47

Graph 27. total generated output power of TEGs with cardboard boxes waste combustion.	48
Graph 28. generated output power of TEGs and heat release rate from cardboard boxes waste combustion with heatsink and with no lateral wind.	48
Graph 29. total generated output power of TEGs with cardboard boxes waste combustion.	49
Graph 30. the generated output power of TEGs and heat release rate from cardboard boxes waste combustion with heatsink and with lateral wind.	50
Graph 31. total generated output power of TEGs with cardboard boxes waste combustion.	50

List of Table

Table 1. The Heating Values of different types of waste in Btu/Ib [30].	14
Table 2. Estimated annual emissions due to open burning of different type of waste [33].	15
Table 3. Fire scenarios proposed for analysis.	18
Table 4. summary of parameters of waste sample for the test input.	19
Table 5. the test result of wood pellets and paper samples [36].	21
Table 6. summary of combustion test result of rubber and trash can.	23
Table 7. results of combustion test of cardboard boxes filled with polystyrene cups.	25
Table 8. Thermal properties of the TEG's materials.	28

Chapter 1

Introduction

1.1 Introduction

The world's energy demand is increasing very rapidly. There are many sources and techniques being invented to fulfil the energy needs. Thermal energy harvesting is a technique that refers to collecting waste heat to put it back into the system. It increases the electrical and thermal efficiency of the system which benefits economic growth and emission reduction. The world is now looking at a variety of methods for introducing thermal energy harvesting systems. Heat to electrical energy conversion is currently an important method for electricity generation [1].

This study approaches the CFD (computational fluid dynamics) modelling to generate electric power through thermoelectric generators (TEGs) from waste combustion. This thermal conversion needs to be done in a curial way, which is affected by numerous environmental conditions. The pattern of heat flow, wind blow, ambient temperature, humidity, and TGE's materials properties are considered to do the FDS (fire dynamic simulator) simulation. FDS is a tool of CFD used to assess the heat release rate from the fire and temperature differences across the TEGs.

1.2 Background

According to the world bank, humankind produces two billion tons of waste per year globally [2]. To deal with them in a sustained way, different approaches are adopted for waste disposal. One of the most extensive uses is incineration, which is commonly applied to a wide range of combustible wastes. While incinerating some combustible materials, thermoelectric generators (TEG) could be applied to produce electric power. In essence, the TEG harvests heat from the burning of combustible wastes lead to a temperature gradient between the main faces of the device which in turn, generates electricity.

1.3 Study motivation

During open incineration processes, enormous heat waste is released to the environment. To take advantage of this generated heat, the waste-to-energy concept can be applied in these types of facilities to convert harvested heat from burning waste into electric energy.

It also provides a suitable solution to deal with the municipal solid waste. Incineration is one of the available and accepted treatment methods of solid wastes globally. There are three main types of waste to which incineration is applied extensively: municipal solid waste, hazardous waste, and medical waste. The combustible municipal waste is composed of paper, paperboard, plastics, rubber, and wood textiles [3]. As shown in the following chart, 11% of total global waste is incinerated. Other common treatment methods of waste are in the form of open dumps (33%), landfill (25%), and recycling (13.5%) [4].

In the European Union, 0.5% of total waste is incinerated without producing energy. The other 40% get recycled, 40% get landfilled and the rest are disposed in the form of backfill and energy recovery [5]. In Spain, 22.2 million tons of municipal waste are produced, among which 11.6% is incinerated. Comparability, this value is higher than other European countries. Thus, 53.4% ended up in landfills, 18% is recycled and only 17% is composted [6].

The basic aim of United Nations (UN) is to discuss common worldwide problems and to find shared solutions that benefit all humanity. In 2015, the UN planned the 2030 agenda for sustainable development, which is composed of 17 goals. The 7th goal is to ensure access to clean and affordable energy [7]. No doubt, this work may contribute to ensure reliability, affordability, and modern energy services for people.

1.4 Objective of study

The main objectives of this work are:

1. To assess the electricity power produced by using TEGs and human-controlled fires from common combustible waste via CFD modelling.
2. To compare the power generation capacity from different types of waste combustion through the TEGs devices.

Chapter 2

Literature Review

2.1 Thermoelectric Generators (TEGs)

2.1.1 About TEG

Thermoelectric generator (TEG) is a solid-state device that produces electrical energy from the temperature gradient. It was invented by a German physicist, Thomas Johann Seebeck in 1821 [8]. It works by the Seebeck effect. Such devices have two dissimilar surfaces with different temperatures to convert that temperature difference into electricity. TEGs provide many advantages like, not having any moving parts, having a long lifetime, unnecessary maintenance, environmental friendliness and simple to design [9]. Unlike other power producing devices thermoelectric generators have very low efficiency [10].

The TEG converts the heat into DC electric power through the **Seebeck effect**. The Seebeck effect happens due to the motion of charge within semiconductors. It produces an electromotive force (emf) across two sides of a charge conductive material when there is a temperature gradient between heat source and heat sink sides. It can be possible due to the doping of P-type and N-type of the semiconductors. In an n-type doped semiconductor, the charge carriers are mostly free electrons, while in a p-type doped semiconductor, the charge carriers are free holes, i.e., missing electrons in the valence band. The **thermocouple** (consisting of a p-type and an n-type semiconductor connected in series by a metal strip) is the basic building block of a TEG [11].

In detail, the TEGs are composed of thermocouples, comprising a pair of P-type and N-type thermoelements or legs connected electrically in series and thermally in parallel. On the cold side, the P-types leg has a positive seebeck coefficient connected with the external terminal to the load as V_1 . While the N-type leg on the cold side have negative seebeck coefficient terminal connected to load as V_2 . The two legs are linked together on one side by an electrical conductor forming a junction or interconnect, usually being a copper strip at the hot side shown in figure [12].

between the TC arms. The temperature difference between the thermocouples has changed [13].

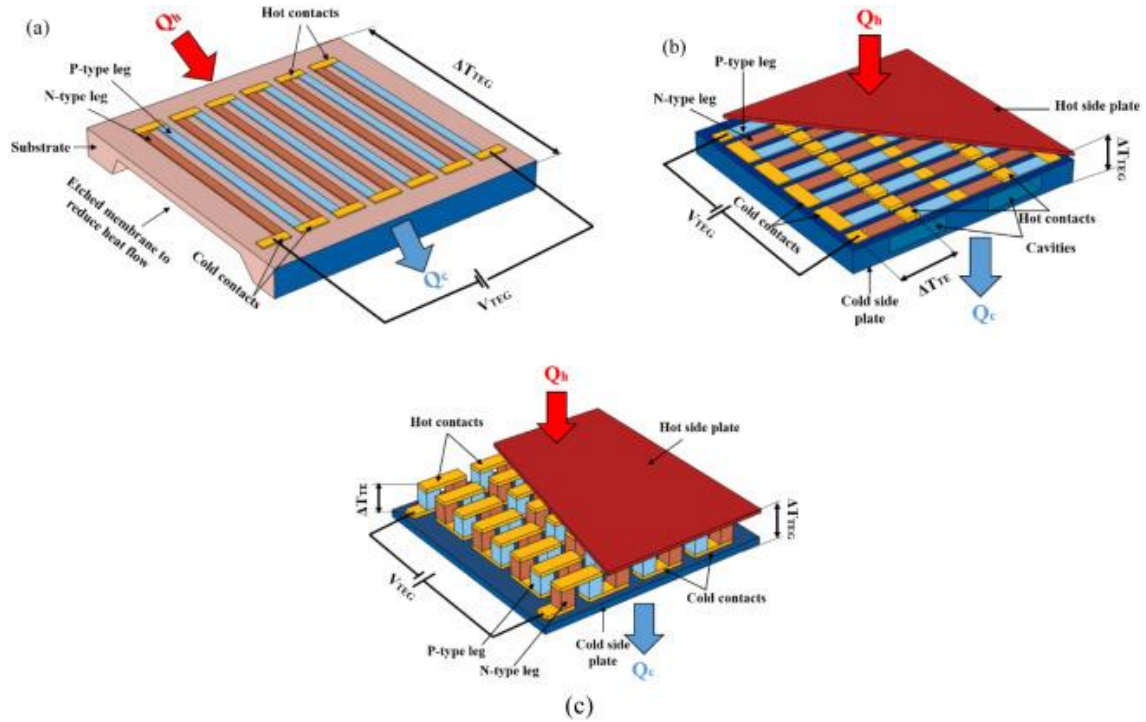


Figure 2. Different designs of TEG, a) lateral type; b) vertical type; c) mixed type.

2.1.2 Materials used to design the TEG.

Thermoelectric electric generator is in a sandwich form. It is composed of different layers of materials. The selection of materials can be done by its different properties, such as seebeck coefficient (α), thermal conductivity (k), electric resistivity (ρ), and absolute temperature (T). The thermoelectric materials figure of merit (ZT) is given below.

$$ZT = \frac{\alpha^2 T}{\rho k}$$

Bismuth telluride (Bi_2Te_3) is a compound that has been extensively used in the construction of thermoelectric modules. The highest ZT value of Bismuth telluride is 0.9 for p-type, and for its value is 0.6. It is clear from equation 01, its value is increased to have a higher seebeck coefficient, smaller resistivity, and a lower conductivity value of materials. ZT is also affected by the temperature [14].

2.1.3 Mathematical modelling of TEG

Thermoelectric generator uses the heat (Q) and converted it into electric power (P) with an efficiency (η),

$$P = \eta Q$$

The output power depends on the amount of heat that can be directed through the thermoelectric materials and frequently depends on the size of the heat exchangers used to harvest the heat on the hot side and reject it on the cold side. The efficiency of a thermoelectric generator depends heavily on the temperature difference across the device. This is because the TEG, like the heat engines, it doesn't have greater efficiency than a Carnot cycle. The efficiency of a TEG is typically defined as follows [15].

$$\eta = \frac{\Delta T}{T_h} \cdot \frac{\sqrt{1+ZT} - 1}{\sqrt{1+ZT} + \frac{T_c}{T_h}}$$

Where the first term is the Carnot efficiency and ZT is the material figure of merit, whose value is obtained from the following expression:

$$ZT = \frac{\alpha^2 T}{\rho \kappa}$$

Here, the Seebeck coefficient (α), the electrical resistivity (ρ), and the thermal conductivity (κ) are temperature (T) dependent materials properties [16].

The performance of TEG depends on some internal factors such as seebeck coefficient, resistivity of materials, thermal conductivity of materials, temperature difference between heat source and heat sink sides, length (thickness), and surface area [17].

$$\text{Heat flow at the hot junction side: } Q_h = 2aIT_h + \frac{2kA}{l} \Delta T - \frac{1}{2} I^2 \frac{2\rho A}{l}$$

$$\text{Heat flow at cold junction side: } Q_c = 2aIT_c + \frac{2kA}{l} \Delta T + \frac{1}{2} I^2 \frac{2\rho A}{l}$$

$$\text{Electric power generation: } P_e = (Q_h - Q_c) = 2aI\Delta T - I^2 \frac{2\rho A}{l}$$

$$\text{Internal resistance: } Ri = \frac{2\rho l}{A}$$

$$\text{Open circuit voltage: } V_{oc} = 2\alpha (T_h - T_c) = ZT(T_h - T_c)$$

short circuit current: $I = \frac{V_{oc}}{R_l + R_i}$

Load voltage: $V = IR_l$

Output power: $P = I^2 R_l$

Whereas.

P = total output power (W)

V = total voltage (V)

Voc = open circuit voltage (V)

I = Short circuit current (A)

Ri = Internal resistance (Ω)

RL = load resistance (Ω)

α = seebeck coefficient ($\mu V/k$)

The = hot side temperature (K)

Tc = cold side temperature (K)

ρ = resistivity of materials ($\mu\Omega m$)

l = Thickness (mm)

A = Area of TEG (mm²)

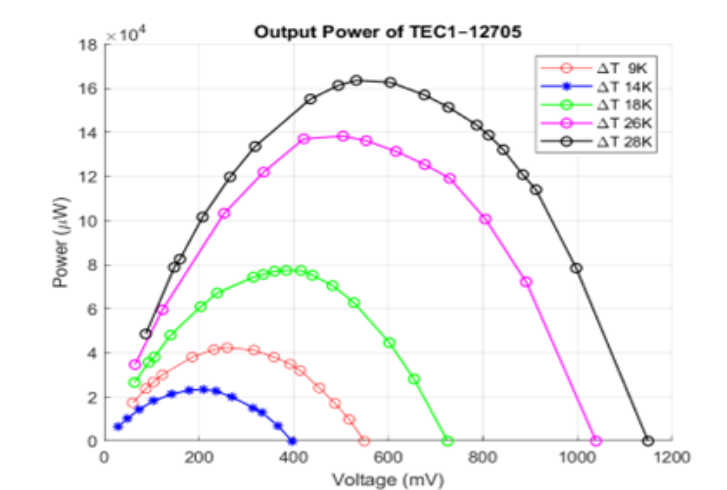


Figure 3. characteristics of output power curve of thermoelectric generator [18].

The voltmeter should directly measure the voltage at two terminals of the TEG, while the ammeter should close the circuit through a potentiometer to measure the current [18]. The output power of TEGs depends on the voltage at the terminal circuit as shown in figure 3. Output voltage is proportional to the temperature difference between hot and cold junction. Higher the temperature gradient of the heat source and heat sink sides of the TEG, higher the voltage at the circuit terminal. The increased temperature difference

between both sides, maximised the optimal output power. The temperature difference is increased when heat supply is higher at the heat source side or is decreased with lower temperature (higher heat remover) at the heatsink side. To achieve optimal power, temperature is continuously increased at the heat source side till a certain point, where the TEG can bear it. Another option is decreasing the temperature at the cold side to get a higher temperature difference. There are different methodologies commonly used to keep it cooler [19].

2.1.4 Cooling systems of TEG

Cooling is an essential aspect to deal with to improve the performance of TEGs. There are several methods and techniques applied for thermoelectric cooling (TEC) systems. Some important techniques are (1) fan heat sink, (2) fin heat sinks, (3) surface-to-air heat dissipation and circulating nanofluid cooling systems, (4) heat pipes with cooling fans for convective heat transfer. Apart from heatsink, some types of coatings could be also used to improve the performance of the TEG. For example, a coating of acrylic polyurethane-based heat reflective coating (Therma cool 0.3M) of 120 μm can be used to considerably reduce the temperature of the cold side, or a thermal paste can be added to the circuit board to get a reduction of at least 20°C [20].

1. **Fan heat sink:** The two possible ways to assemble the cooling system to airflow uses in forced convection, (a) top fan-cooling system and (b) side fan-cooling system are shown in fig. 4. The top-mounted fan cooling system requires a fan in every certain number of TEG, usually one or multiple TEGs depending on the fan size. On the other hand, in the side-mounted fan system, the airflow generated by a fan flow through one or multiple heat sinks depending on the number of TEGs. The outlet air temperature of a preceding TEG is lower than the cold side temperatures of following TEGs as long as the initial air temperature is lower than a hot side temperature. It enables us to create enough temperature difference on the following TEG and results in electricity generation. The top-mounted fan (TMF) system is more affected to has lower cold side temperature when it has more than one TEG [21].

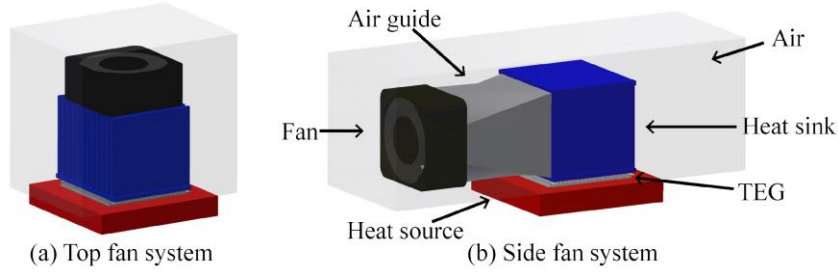


Figure 4.(a) top-mounted fan (TMF) and (b) side-mounted fan (SMF).

2. **Fin heat sinks:** The fin heat sink is another method for the cooling of TEG. The fin arrangement and the convection heat transfer coefficient represent the most effective parameters on thermal resistance. The selection of the optimum number of fins and fins gap of the heat sink for certain air speed along the length of the fins help to design optimum performance of the fins. There are two types of fins heat sink used to airflow for cooling the TEG. The round pin and rectangular fins are shown fig 5. The rectangular one is mostly used among these profiles alongside multiple fin arrays. The round pin heat sinks are characterised by omnidirectional features and are mostly preferred with low airflow or when its direction of flow is unknown [22].

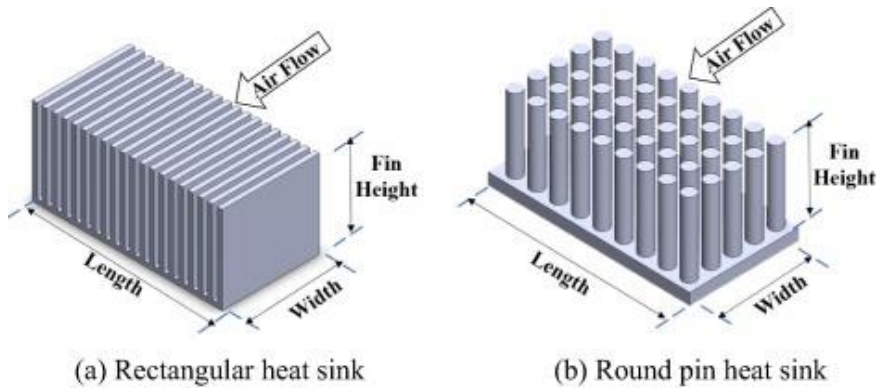


Figure 5. Diagrams illustrating rectangular and round pin heat sink [22].

3. **Fluid cooling heat sink:** the fluid cooling heat sink system is illustrated in the fig. 6. The cooling fluid takes the heat in the heat sink and flows to liquid cabin. The hot water is pumped to the condenser and get cooled then returns to the heat sink. The nanofluids were used as coolants for the cold side to enhance the conversion capability of the TEG system. Due to the relatively high specific heat capacity of the coolant, the temperature variation of the coolant is negligible. The inlet temperature of the coolant is set to 303 K. In case of air-fluid instead of pump the compressor is used [23].

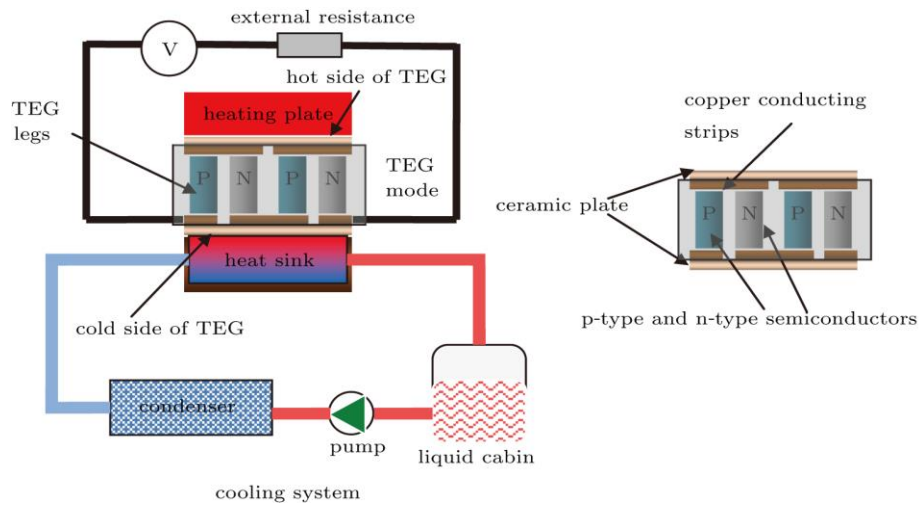


Figure 6. Schematic diagram of the TEG model and fluid cooling structure.

2.1.5 Applications of TEGs

- For industrial uses:** After the discovery of thermoelectric effects, the innovation of TEGs has been started. The first TGE (piles) model was presented by M.G Farmer in Paris 1867, but in this century, it was never used for industrial purposes. Later, in 20th century, TEGs were widely used for many industrial, space, and medical fields. The early TEGs were mostly used in industrial field for electro-depositing, electro-plating, charging secondary devices, electric lighting, telegraphic and electro-plating, and for others electronic devices [24].
- For electric generation:** Thanks to bismuth telluride and alloys materials for having the maximum operating temperature (550-900K), made able TEGs for electricity generation. The power generation by TEGs from recovery of waste heat in different sectors are mainly categories into autonomous and industrial. TEGs are being developed as autonomous power sources to turn the exhaust gas heat into low power (5 μ W to 1 W) and high power about 1 kW. In the industrial heat recovery system, 10% - 20% waste heat can be turned into electricity depending on the temperature of flue gases, number of TEG units and environmental conditions. The TEGs are placed on the exhaust gas pipeline to convert the heat into electric power with different range [25].

2.2 Potential heat sources from wastes and biomass

2.2.1 Waste generation worldwide

Globally, the rate of waste generation is rising annually. In 2020, the world was estimated to generate 2.24 billion tonnes of solid waste. The annual waste generation is expected to increase by 73% from 2020 levels to 3.88 billion tonnes in 2050. It is because of more urbanisation and rapid growth of population [26].

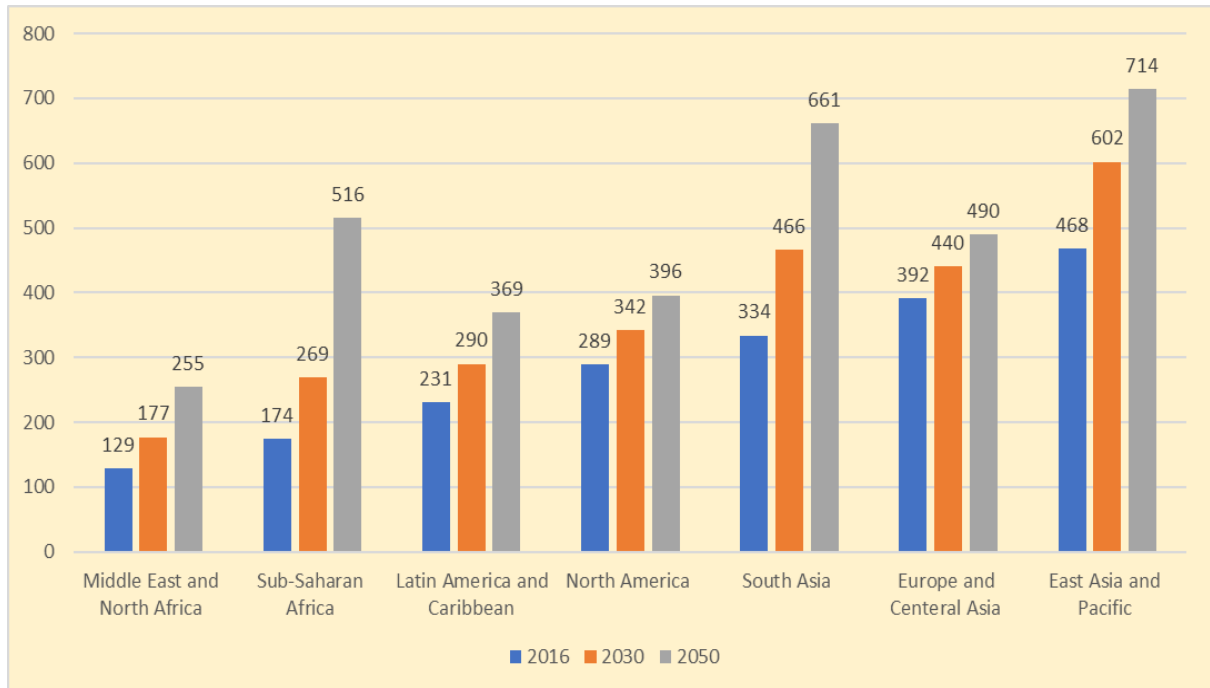


Figure 7. waste generation, by region (millions of tons/years) [26]

The total quantity of waste generated in low-income countries is expected to increase by more than three times by 2050 shown fig.7. The East Asia and Pacific region are generating most of the world's waste, at 23 %, and the Middle East and North Africa region is producing the least in absolute terms, at 6 %. However, the fastest growing regions are Sub-Saharan Africa, South Asia, and the Middle East and North Africa, where, by 2050, total waste generation is expected to more than triple, double, and double respectively [26].

2.2.2 Waste materials

There are different types of waste, and their compositions are food and green waste (44 %), paper and cardboard (17 %), plastic (12 %), metal and glass (9 %), rubber and leather (2%), rest (14 %) shown in the fig. 8. [26]. The interesting aspect is that most of them are combustible waste. They can be burnt to produce the electricity.

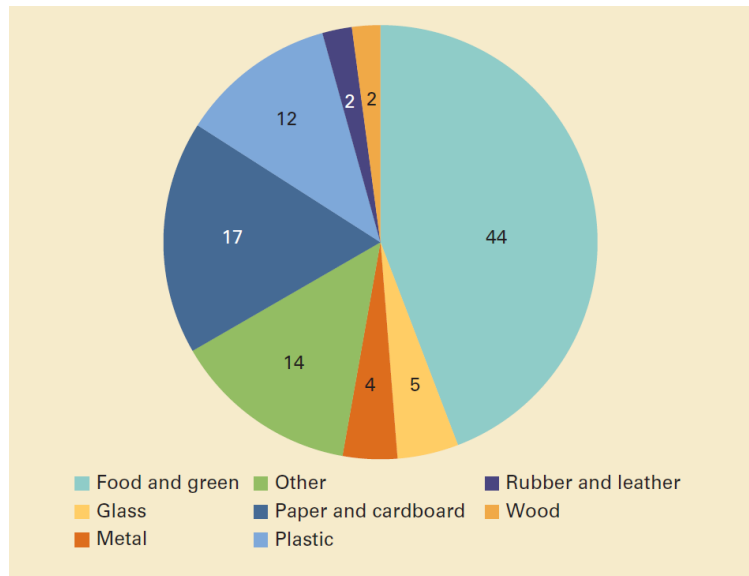


Figure 8. Global waste composition (percent) [26]

2.2.3 Waste management

The effective waste management methods can be adopted in terms of economic and environmental aspects. Waste minimisation, reuse, recycling, sustainable landfill, disposal techniques and energy recovery are the most effective ways to deal with different types of waste. Mostly construction and electronic waste are preferred to be recycled and reused respectively. After their end use, they are dumped openly along with other metal and plastic wastes. The major processes involved in energy recovery from waste are anaerobic digestion, gasification and pyrolysis, and incineration. To avoid combustion, the organic wastes are used through the gasification and pyrolysis processes to produce methane and hydrogen gas with unwanted emission CO₂ and CO. The other combustible wastes (dried organic waste, wood waste, paper and cardboard, rubber, etc.) are burnt in a moving grate by incineration process to produce heat, flue gas, and ash. The grate incinerator has up to 1000 °C temperature to produce the steam for electricity generation [27].

In waste management, incineration is one of the available accepted treatment methods of solid waste globally. There are three main types of waste to which incineration is applied extensively: municipal solid waste, hazardous waste, and medical waste. The combustible municipal waste is composed of paper, paperboard, plastics, rubber, wood textiles, and so on [26]. As shown in the following fig. 9, 11 % of total global waste is incinerated. Other common treatment methods of waste are in the form of open dumps (33%), landfill (25%), and recycling (13.5%) [27].

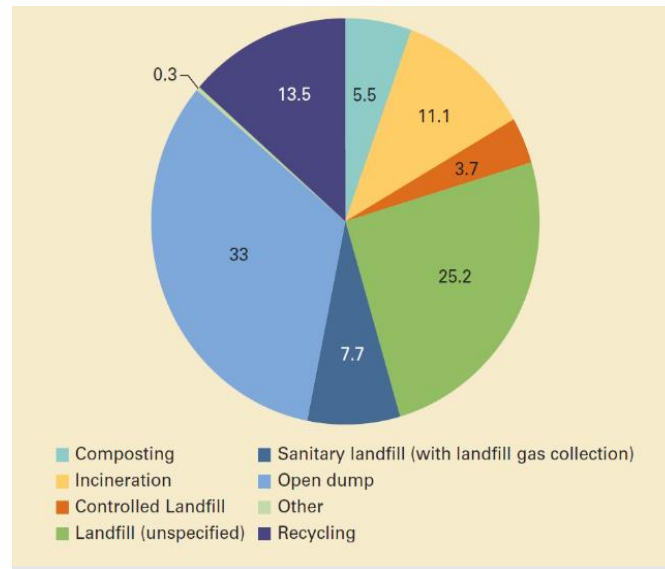


Figure 9. global waste treatment method

The temperature of the waste incineration mainly depends on the type of waste; its composition and physical/chemical characteristics different processes and facilities are used. Incineration temperatures of a mixture of solid waste is from 900 to 1300 °C when the rotary kilns are used. The liquid waste is burnt via banners in liquid-injection furnaces in chambers at temperatures of usually 1000 °C and higher. In fluid bed furnaces, the (solid or liquid) waste substances must be incinerated to get up to 900 °C. The temperature in the combustion chamber, fixed grate furnaces is on average 600-1000 °C [28].

In the EU, 0.5 % of total waste is incinerated without producing energy. The other 40 % get recycled, 40 % get landfilled and the rest are disposed of in the form of backfill and energy recovery [29]. In Spain, 22.2 million tons of municipal waste of which 11.6% is incinerated is given in following figure. This value is higher compared to other countries in Europe. Another 53.4% ended up in landfills. 18% is recycled only and 17% is composted [30].

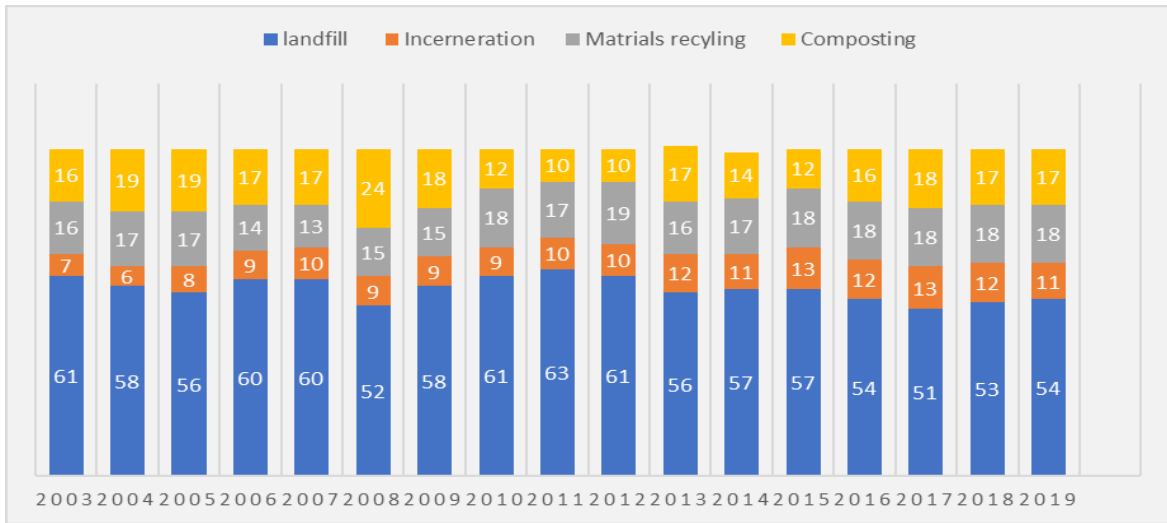


Figure 10. Solid waste treatment methods in Spain [30]

2.2.4 Heating values of waste

The efficiency of waste combustion is dependent on heating value and technologies of incineration. Further heating value of waste depends on its ignition temperature, flash point and flammability, moisture content and so on. The range of waste's heating value (HV) is 2,500 Btu/lb to 10,000 Btu/lb is given in the table below. Industrial wastes containing heavy construction waste, carpentry and floorwork and paint preparing waste etc. have higher HV. From fig.8, 25% of total global wastes are generated from the open areas and having 6,500 Btu/lb HV [31].

Source	Types of waste	Heating Value (Btu/lb)
Residential	Rubbish and garbage	4,300
Industrial	Heavy Construction: Asphalt wastes, used oil etc. Carpentry and Floorwork: Acetone, adhesives, coatings, methylene chloride, methyl ethyl ketone (MEK), toluene, treated wood, trichloroethylene, and xylene Paint Preparation and Painting;	10,000
Open Areas	Combustible waste, paper, cartons, rags, wood scraps, rubber, combustible floor sweepings	6,500
Commercial	Animal and vegetable wastes; restaurants, hotels, markets; institutional, commercial, and club sources	2,500

Table 1. The Heating Values of different types of waste in Btu/lb [30].

2.2.5 Emissions from waste combustion

There are many noxious emissions and products of open burning of waste. The exact emissions from a waste fire can range depending on the burning conditions (temperature, environment, location etc.) and on its composition. Most effective common emissions are listed in the table below.

Pollutants	Global Emission due to open burning (kg/year)	% of total global emissions of pollutant
Carbon Dioxide (CO ₂)	1.4 trillion	5
Methane (CH ₄)	3.6 billion	1
Coarse Particulates (PM ₁₀)	12 billion	24
Fine Particulates (PM _{2.5})	10 billion	29
Black Carbon (BC)	632 billion	11
Carbon monoxide (CO)	37 million	7

Table 2. Estimated annual emissions due to open burning of different type of waste [33].

It shows yearly emissions of CO₂ which is estimated to be 1.4 billion tons per year this figure accounts for only about 5% of total global CO₂ emissions. The estimation of methane gas production due to open burning of waste is 3.6 million tons per year or only 1% of total global methane emissions. Carbon monoxide (CO) is a greenhouse gas that can be very harmful to humans when inhaled. Open burning of waste produces an estimated 37 million tons per year of CO gas. Particulate matter (PM), the primary component of air pollution, is produced in large quantities when waste is burned openly, and it can be released into the air through smoke. The estimated yearly emissions of PM₁₀ due to open burning of waste is 12 million tons/year. Additionally, PM_{2.5} and black carbons are particulate matter emissions that contribute 29% and 11% to global emissions respectively [32].

2.2.6 Emission control methods

These flue gases are not acceptable for the environment. Their treatment, cleaning and cooling or elimination must be carried out during incineration of waste. The flue gas treatment and cleaning methods differ strongly. Flue gases are usually cleaned from the particulate matter (PM) by using an electrostatic precipitator, lime injection, fabric filter, wet scrubber, or combinations thereof. Another option is cooling the flue gases in a boiler or using an evaporation cooler. The treatment of flue gases by means of quenching them

from high temperatures down to below 200 °C. The detention time of the gases between 400 and 200 °C is then minimal [33].

The following figure.11 is Amine-grafted, a technology used to capture the CO₂ from flue gases after combustion. The adsorption of CO₂ is achieved through acid–based interactions between the CO₂ and the amines. For amine-based adsorbents, different types of amines (primary, secondary, and tertiary) have been immobilised within the pores of solid supports. The adsorption of CO₂ is achieved through acid–based interactions between the CO₂ and the amines [34].

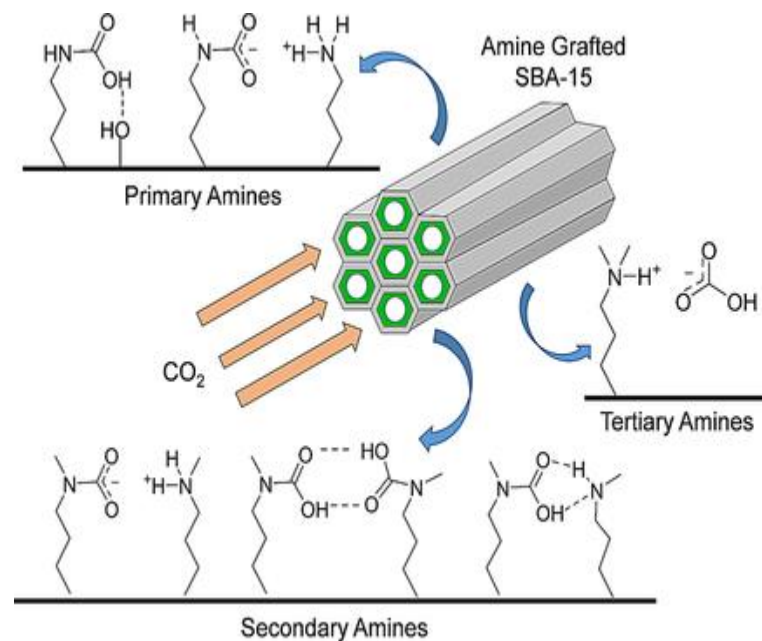


Figure 11. Amine-grafted [34]

Fabric filters are used for removal of particulate matter and black carbon from flue gases. It is shown fig.12 the dirty gas containing PM is sucked through a fabric filter bag below-side. The fabric bag collects the dust, which is removed periodically by shaking the bag. At the top the cleaned gases are left into air and collected dust are separated from the bottom. Fabric filters can be very efficient collectors for even submicrometric-sized particles and are widely used in industrial applications, although they may be sensitive to high temperatures and humidity [35].

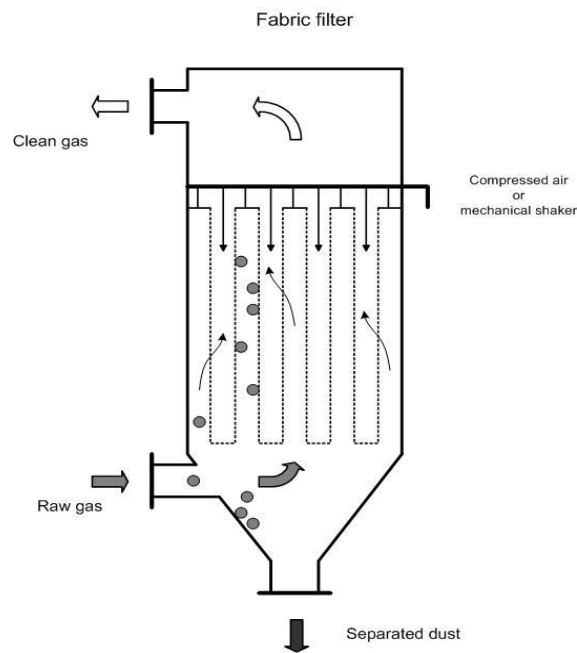


Figure 12. fabric filter [35]

Chapter 03

Methodology

3.1 Data collection

After reviewing many previous research papers, the conclusion is that wood pallets, paper, rubber trash can, and cardboard box wastes have quite good heating value. These are very commonly available types of wastes; their selections are suitable for this study. The following tables describe some proposed fire scenarios of these wastes. Some essential data were collected from the experiment in the National Fire Research Laboratory for CFD simulation.

The 12 proposed fire scenarios are given in table 03. Burning of three different types of waste (wood pallets, rubber trash can and cardboard boxes) are chosen as heat sources. The burning of each type of waste are assumed to be carried out into four different situations (without heatsink with on lateral wind, without heatsink with lateral wind, with heatsink with no lateral wind, and with heatsink with lateral wind).

Scenario	Fire source	Heat sink	Lateral wind
1	wood pallets	no	no
2	rubber trash can	no	no
3	cardboard boxes	no	no
4	wood pallets	no	yes
5	rubber trash can	no	yes
6	cardboard boxes	no	yes
7	wood pallets	yes	no
8	rubber trash can	yes	no
9	cardboard boxes	yes	no
10	wood pallets	yes	yes
11	rubber trash can	yes	yes
12	cardboard boxes	yes	yes

Table 3. Fire scenarios proposed for analysis.

The experimental burning of waste samples was done by the National Fire Research Laboratory-NIST. This study considered the results of these experiments and used them for CFD simulation. Some important parameters such as size, weight, and net heat of combustion of selected waste samples are measured before performing the test. The values are summarised in the following table 04.

Summary for Test Input							
	Wood Pallet & paper		Rubber trash can		cardboard boxes filled with polystyrene cups		
Parameters	Value	Uc	Value	Uc	Value	Uc	Unit
Fuel types	Cellulose	–	Plastic	–	Cellulose, Polystyrene	–	
Hood Size	6	–	3	–	9	–	m
Effective Duct Diameter	1.975	0.005	0.485	0.005	1.975	0.005	m
Exhaust Flow Correction Factor	1.028	0.029	1.033	0.029	1.028	0.029	–
Net Heat of Combustion (per unit mass O ₂), E _f	13.61	0.41	13.1	0.66	13.1	0.66	MJ/kg
Net Heat of Combustion (per unit mass fuel), HOC _f	16.12	0.6	30	6	25	5	MJ/kg
Initial Specimen Mass, M _i (gravimetric)	136.25	0.02	5.04	0.02	56	0.02	kg
Final Specimen Mass, M _f (gravimetric)	6.55	0.02	0.2	0.02	0.11	0.02	kg

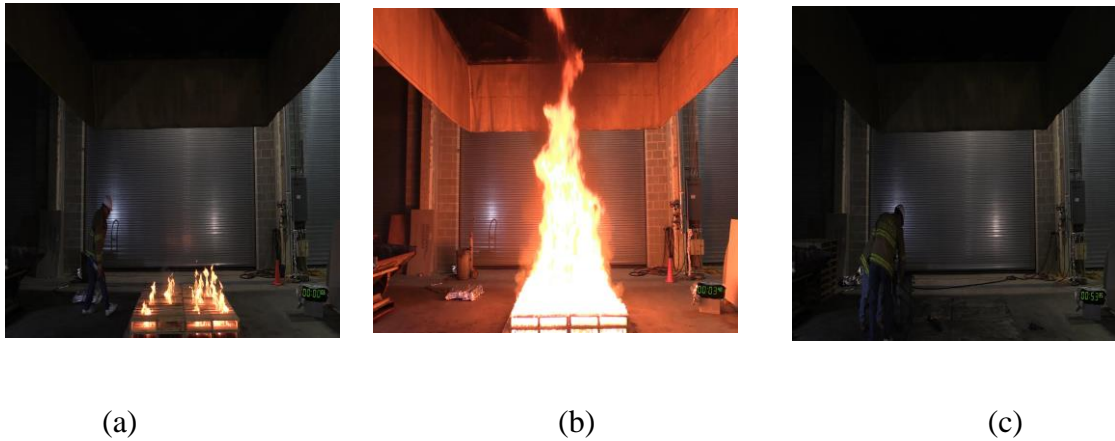
Table 4. summary of parameters of waste sample for the test input.

3.1.1 Combustion of the wood pallet and paper

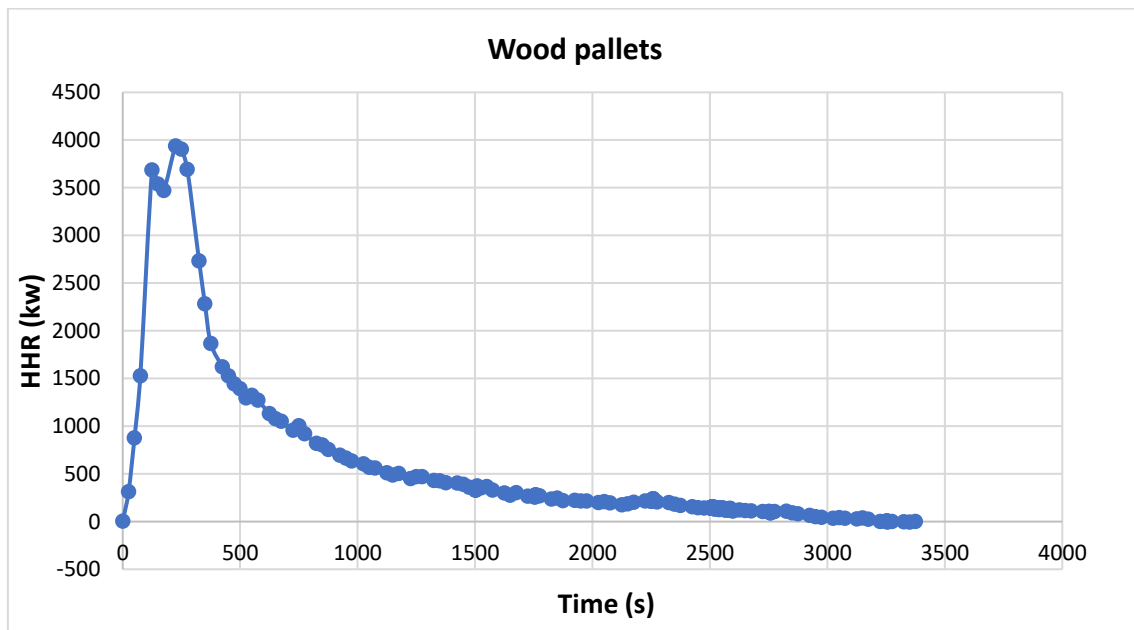
The sample wood pallets and paper are burnt to perform the combustion test in the NIST laboratory [35]. The test input parameters of the sample are given table 2. The performance of the experiment is shown in figure 13.

- (a) The sample just started to get burnt.
- (b) The fire is at peak level.
- (c) When sample is completely burnt

Figure 11 combustion test process of wood pellets and paper sample



The 136.25 kg weight and 6 metre size of wood pellet and paper sample took 52 minutes to burn completely. The total heat release rate of combustion is indicated in the following graph. After three minutes of ignition the peak value of heat release rate is noted.



Graph 1. heat release rate from wood pellets combustion.

The results of the experiment (wood pellet and paper combustion) are summarised in table 05. Peak heat release rate is 4171 kW and total heat release rate is 2230.6 MJ. It is noted that 0.06 kg CO₂ is produced by burning one kg of wood pellet.

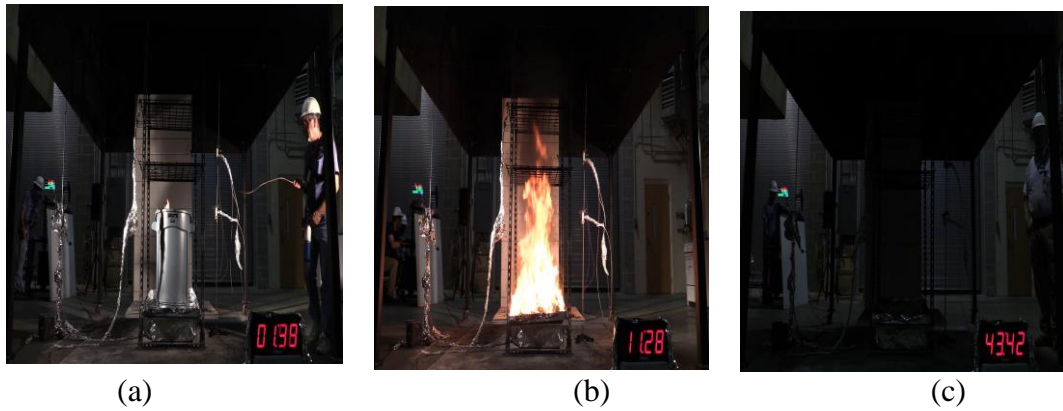
Summary of test results			
Measurement	Value	Uc	Unit
Peak Heat Release Rate, PHRR	4174	182	Kw
Time to Peak Heat Release Rate	3.72	0.17	Min
Total Heat Released, THR	2230.6	105	MJ
Natural Gas Burner Total Heat Released, NGTHR	0	–	–
Heat Release Quality Confirmation, HRQC	–	–	–
Net Specimen Mass (gravimetric), NM = Mi-Mf	129.7	0.028	Kg
Net Effective Heat of Combustion = THR / NM	17.19	0.81	MJ/kg
O2 Yield = O2 Consumed / NM	1.273	0.041	kg/kg
CO2 Yield = CO2 Generated / NM	1.658	0.06	kg/kg
CO Yield = CO Generated / NM	0.0322	0.0012	kg/kg
Soot Yield = Soot Generated / NM	0.00388	0.00057	kg/kg
Baseline Hood Exhaust Flow	25.49	0.76	kg/s
Test Duration = Time (Fire Out) - Time (Ignition)	53.47	0.03	Min

Table 5. the test result of wood pellets and paper samples [36].

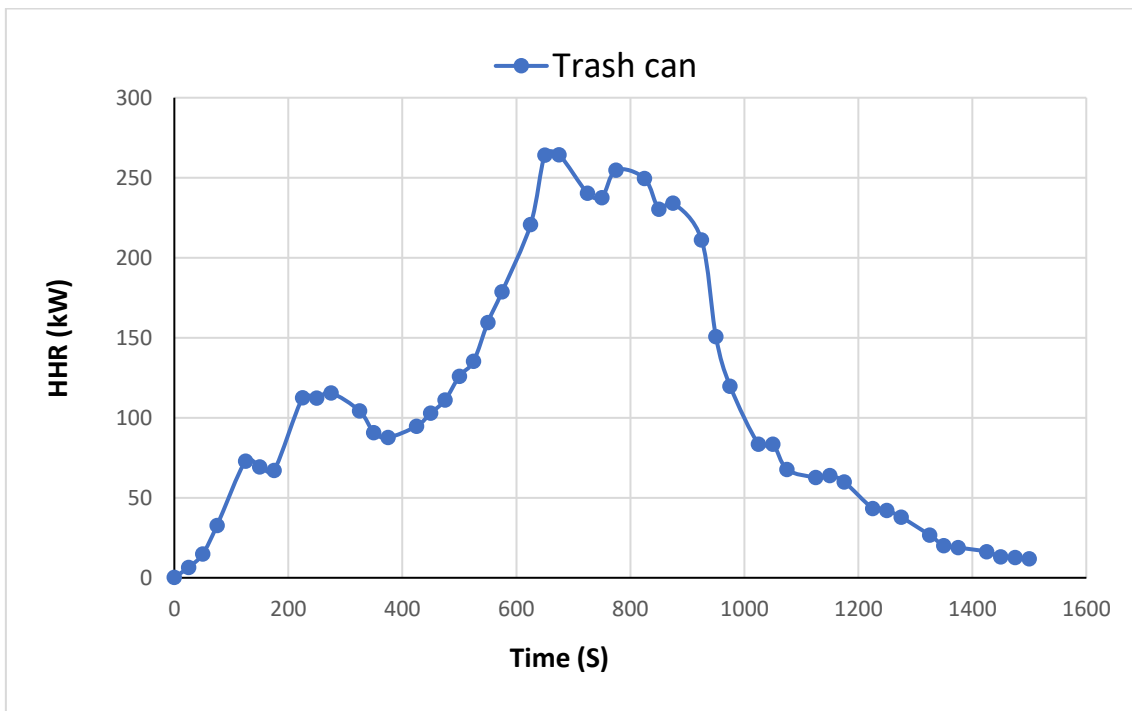
3.1.2 Combustion of rubber trash can

Procedure of burning a rubber trash can sample is mentioned in figure 14. A very light-weight 5 kg and size 3 metre sample is burnt completely after 43 minutes. The steps of the experiment are shown as: ‘a’ being the starting point of ignition, after which we started noticing the time. Then, during point ‘b’ the peak heat release rate is noted during the combustion and at ‘c’ time and heat release rate were noted when the combustion is over.

Figure 12. combustion test process of rubber trash can sample.



Total heat release data with time is shown in the following graph. The peak heat release rate is noted at 11.28 minutes. The combustion is over after 25 minutes.



Graph 2. heat release rate from rubber and trash can combustion.

Table 06. shows the output values of test results. Total 167 MJ heat is released when the rubber trash can sample is burnt completely after 25 minutes. 280 kW is noted as peak heat release rate after 11 minutes of its' ignition. 2.6 kg CO₂ is produced when one kg of sample is burnt.

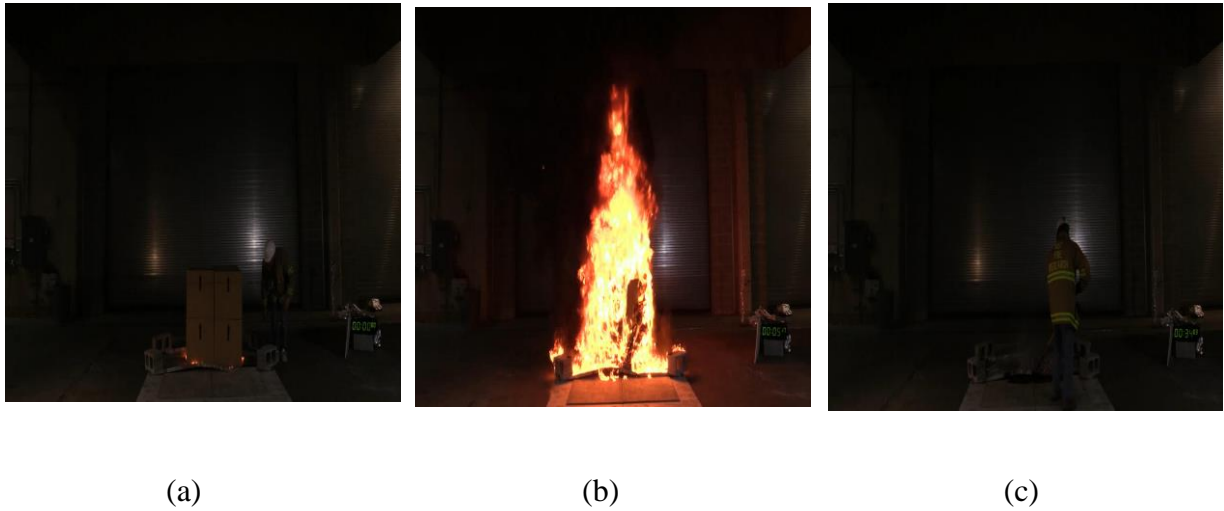
Summary of test results			
Measurement	Value	Uc	Unit
Peak Heat Release Rate, PHRR	281	17	kw
Time to Peak Heat Release Rate	11.48	0.17	min
Total Heat Released, THR	167	10	MJ
Natural Gas Burner Total Heat Released, NGTHR	-1	–	MJ
Heat Release Quality Confirmation, HRQC	–	–	–
Net Specimen Mass (gravimetric), NM = Mi-Mf	4.844	0.028	kg
Net Effective Heat of Combustion = THR / NM	35.2	2.2	MJ/kg
O2 Yield = O2 Consumed / NM	2.578	0.048	kg/kg
CO2 Yield = CO2 Generated / NM	2.639	0.096	kg/kg
CO Yield = CO Generated / NM	0.01761	0.00064	kg/kg
Soot Yield = Soot Generated / NM	0.00332	0.00051	kg/kg
Baseline Hood Exhaust Flow	3.125	0.094	kg/s
Test Duration = Time(Fire Out) - Time(Ignition)	43.68	0.03	min

Table 6. summary of combustion test result of rubber and trash can.

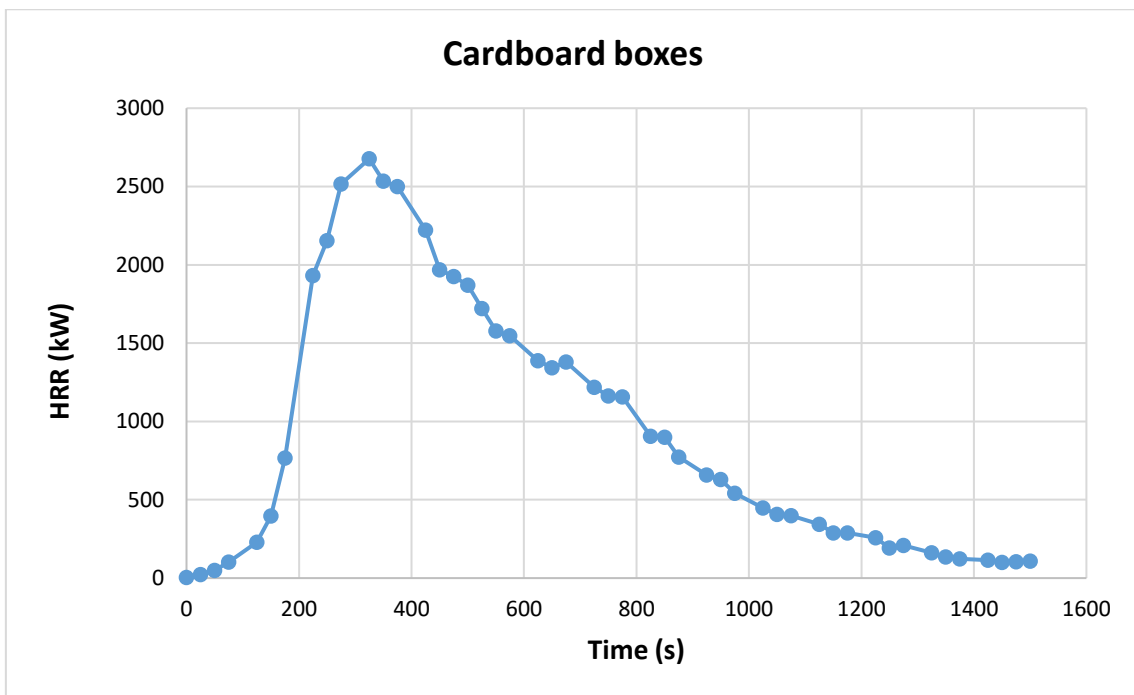
3.1.3 Combustion of cardboard boxes filled with polystyrene cups waste.

The combustion process of the cardboard boxes sample was performed in the NIST laboratory are shown in figure 15. Like previous experiments, the burning of this sample was from start of ignition, ignition is at peak, and end of ignition are shown in (a), (b), and (c) respectively.

Figure 13. combustion test process of cardboard boxes sample.



Following graph is derived after completing the whole combustion test of the sample. It shows the heat released rate over time. The sample was completely burnt at 25 minutes. Peak heat release rate is noted at 5.33 minutes after ignition.



Graph 3. heat release rate from cardboard boxes combustion

The results of the combustion of cardboard boxes sample is given in table 07. The total is 1423.98 MJ heat is released when 56 kg of sample is burnt completely after 25 minutes

time duration. After 5 minutes its ignition 2828 kw peak heat is released. 2.17 Kg carbon dioxide production is noted for per kg of sample burning.

Summary of test results			
Measurement	Value	Uc	Unit
Peak Heat Release Rate, PHRR	2828	171	kw
Time to Peak Heat Release Rate	5.33	0.17	min
Total Heat Released, THR	1423.98	92	MJ
Natural Gas Burner Total Heat Released, NGTHR	1	–	MJ
Heat Release Quality Confirmation, HRQC	–	–	–
Net Specimen Mass (gravimetric), NM = Mi-Mf	55.89	0.028	kg
Net Effective Heat of Combustion = THR / NM	25.7	1.7	MJ/kg
O2 Yield = O2 Consumed / NM	1.942	0.062	kg/kg
CO2 Yield = CO2 Generated / NM	2.172	0.078	kg/kg
CO Yield = CO Generated / NM	0.0566	0.002	kg/kg
Soot Yield = Soot Generated / NM	0.085	0.011	kg/kg
Baseline Hood Exhaust Flow	49.9	1.5	kg/s
Test Duration = Time(Fire Out) - Time(Ignition)	25	0.03	min

Table 7. results of combustion test of cardboard boxes filled with polystyrene cups.

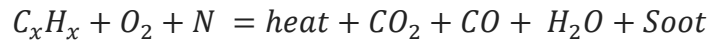
3.2 CFD analysis

Computational Fluid Dynamic (CFD) a type of analysis that helps into solving complex problems and allows the engineers to test the effects of fluid flow on any model. These measurements are done without the need to conduct real-world experiments. The FDS is used as tool for CFD analysis in this study. The basis of twelve proposed scenarios of TEG system discussed at the beginning of this chapter their simulations are done by FDS.

3.2.1 Computational Fluid Dynamic (CFD) models

It is supposed that the modes of heat transfer (convection, conduction, and radiation) happen when we are dealing with waste combustion. The total heat transfer from the combustions in of modes turbulence flow, and radiation, are measured by CFD. Some fire CFD codes (mentioned below in the selection of CFD simulation assumption) are made to identify heat flow from fire to TEGs boundaries by using some following models.

- 1) **Combustion:** In Mixing-controlled combustion model is approached for this study. The combustible waste mainly consists of carbon, hydrogen, oxygen, and nitrogen elements that react with oxygen in presence of air to produce the heat with CO_{YIELD} and $SOOT_{YIELD}$. The simple chemistry model is applied for combustion reaction [37].



In this thesis all chosen combustible waste are composed of hydrocarbons (C_xH_x) is burning with air to produce same products with different values.

- 2) **Turbulence:** Large Eddy Simulation (LES) model is applicable for turbulence flow. The fire plume surrounded a boundary, turbulence flow is occurred during waste combustion. FDS simulation uses this model of turbulent flows by numerically solving the RANS equation requires resolving a very wide range of time and length scales, all of which affect the flow field [38].
- 3) **Radiation:** The radiative heat transfer occurs during the combustion of waste. The DOM model is used by default in FDS to solve the radiative heat transfer equations through the 100 solid angles. The DOM model uses following equation of radiative heat transfer [38].

$$q_r = k(4I_b - G) \quad \therefore I_b = \sigma T^4$$

where G is the total irradiance, κ is the Planck absorption coefficient and I_b is the black body radiation intensity, σ is the Stefan-Boltzmann constant and T is temperature.

- 3.2.2 **Wind:** In the study, the lateral wind existence is considered for some fire scenarios discussed in table 03. The atmospheric wind conditions are modelled by default in FDS simulation. In fire scenarios assumed wind velocity is given in FDS assumption section. The atmospheric wind conditions are modelled by

default in FDS simulation through the Wind Profile Power Law $\left(\frac{u}{u_r} = \left(\frac{z}{z_r}\right)^\sigma\right)$ [39].

3.2.2 Assumptions for FDS (Fire Dynamics Simulator) simulation

Following assumptions are made before the FDS simulations.

- TEGs are built with Bismuth Telluride (Bi_2Te_3) as it is the most used material for these devices.
- The Bismuth Telluride is sandwiched between two aluminium nitride (AlN) plates and a thin layer of copper (Cu)
- The fire source is 30 cm separated from the TEG wall to avoid the flame impingement and thus, to allow the proper operation of the devices (the occurrence of flame impingement could melt the devices)
- Some scenarios include the presence of external wind with a ‘top hat’ profile that blows against the back of the TEG wall with a wind velocity of 3 m/s (average wind speed in Madrid city). An ambient temperature of 20°C is assumed throughout the model.
- The computational domain is defined with cells of 5 cm³ throughout the entire model.
- Heat sinks are assumed to be of aluminium as it is a common and less expensive material.
- Fire scenarios will consist of a combustible material of 0.8 m x 0.8 m x 0.2 m located in the middle of an open computational domain. Next to the fire source, there will be a wall TEGs of 1 m (width) x 2 m (height) composed by a total of **32 TEG** devices, whose dimensions are **20 cm x 20 cm x 5 cm**.
- The combustion reaction of **wood pellets fuel**: C=1.0, H=1.7, O=0.72, N=1.0E-3, CO_YIELD=0.0322, SOOT_YIELD=3.88E-3, HEAT_OF_COMBUSTION=1.719E+4
- The combustion reaction of **rubber and trash cans fuel** (C_2H_4): CO_YIELD=0.01761, SOOT_YIELD=3.2E-3, HEAT_OF_COMBUSTION=3.52E+4
- The combustion reaction of **cardboard boxes fuel** (C_8H_8): CO_YIELD=0.0566, SOOT_YIELD=0.085, HEAT_OF_COMBUSTION=2.57E+4
- Number of output dumps per calculation (NFRAMES=750)
- Simulation ended time (TIME T_END=1500.0)

- **Heat Sink:** RGB=0,51,153, BACKING='VOID', MATL_ID(1,1)='Aluminium', MATL_MASS_FRACTION(1,1)=1.0, THICKNESS(1)=0.05
- **Lateral Wind:** RGB=26,204,26, VEL=-3.0
- **Vent parameters:** VENT_ID='Fire', SURF_ID='Waste Types', XB=-0.9, -0.5,0.3,0.7,0.05,0.05, RGB=255,51,51, TEXTURE_ORIGIN=0.0,0.0,0.05
- **Slice file parameters (SLCF):** SLCF QUANTITY='TEMPERATURE', PBY=0.1, SLCF QUANTITY='TEMPERATURE', PBY=0.35, SLCF QUANTITY='HRRPUV', VECTOR=.TRUE., PBY=0.5, SLCF QUANTITY='TEMPERATURE', PBY=0.5, SLCF QUANTITY='VELOCITY', VECTOR=.TRUE., PBY=0.5, SLCF QUANTITY='TEMPERATURE', PBY=0.6, SLCF QUANTITY='TEMPERATURE', PBY=0.85, SLCF QUANTITY='TEMPERATURE', PBZ=0.15, SLCF QUANTITY='TEMPERATURE', PBZ=0.4, SLCF QUANTITY='TEMPERATURE', PBZ=0.65, SLCF QUANTITY='TEMPERATURE', PBZ=0.9, SLCF QUANTITY='TEMPERATURE', PBZ=1.15, SLCF QUANTITY='TEMPERATURE', PBZ=1.4, SLCF QUANTITY='TEMPERATURE', PBZ=1.65, SLCF QUANTITY='TEMPERATURE', PBZ=1.9

3.2.3 Dimensions and properties of material for TEG.

Power assessment can be done through thermoelectric generators. Its materials compositions and their thermal properties can affect the output generated power. The following table describes the properties of different materials used for TEGs designing.

	Layer 1	Layer 2	Layer 3	Layer 4	Layer 5
Material	Aluminium	Copper	Bi ₂ Te ₃	Copper	Aluminium
Thickness	1 mm	0,5 mm	3 mm	0,5 mm	1 mm
Density	2.707 kg/m ³	8.800 kg/m ³	7.600 kg/m ³	8.800 kg/m ³	2.707 kg/m ³
Specific heat	0.83 kJ/kg·K	0.376 kJ/kg·K	0.165 kJ/kg·K	0.376 kJ/kg·K	0.83 kJ/kg·K
Area	400 cm				

Table 8. Thermal properties of the TEG's materials.

3.2.4 TEGs' arrangements on CFD model

Total 32 TEGs devices made from above materials are combined on a sheet are shown in following figures. This 3-D model is made to consider the above assumption for CFD simulations. The fire source is 30 centimetres separated from the TEG wall to avoid the flame impingement and to allow the proper operation of the devices (the occurrence of flame impingement could melt the devices). The TEGs sheet is also little far from the back side wall to provide a proper cooling to TEGs for a better performance.

The slice file figure 14 from CFD simulation indicates the heat release rate distribution across the TEGs from the waste combustion. On the other hand, the radiative heat distribution in boundaries of TEGs is show in figure 15. It is observed during the whole combustion period that the TEGs on middle columns receive higher radiation and heat.

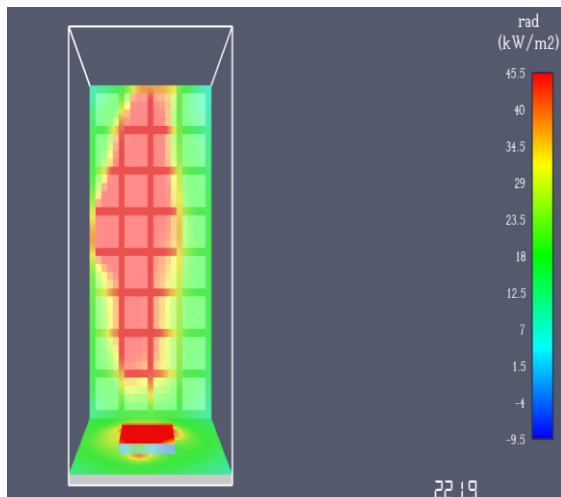


Figure 15. radiative heat distribution in boundaries.

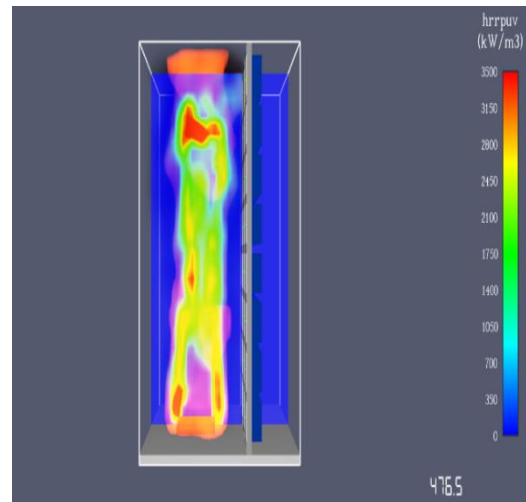


Figure 14 The slice file of heat release rate from waste combustion obtained from CFD.

3.2.5 Output Power Calculation of TEGs.

The temperature of hot and cold faces of TEGs is known from CFD simulations and then we could calculate the temperature gradient across the TEG. Finally, the following steps are used to assess the output power of TEGs [39].

Step1: having temperature gradient and seebeck effect, V_{oc} can be calculated by using following equation.

$$V_{oc} = 2\alpha (T_h - T_c)$$

Step2: From below given equation, Internal resistance of TEG is calculated by using its properties.

$$R_{TEG} = \frac{\rho L}{S}$$

step3: Calculate the maximum output power for each TEG individually [36].

$$P_{TEG,i} = \frac{V_{OC,i}^2}{4R_{TEG,i}}$$

Step4: Calculate the maximum output power of the installation by assuming that the TEG's are connected in series [36].

$$P_{Total} = \frac{(V_{OC,1} + V_{OC,2} + \dots + V_{OC,32})^2}{4(R_{TEG,1} + R_{TEG,2} + \dots + R_{TEG,32})}$$

Chapter 04

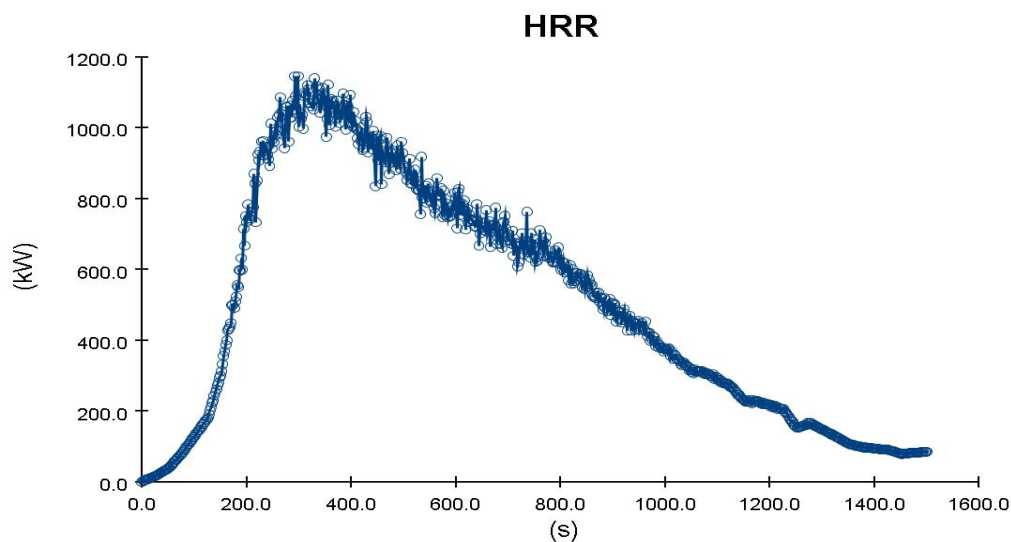
Results and Conclusion

4.1 FDS Results

By using the CFD simulation thermal behaviour of waste fire and its interaction with TEGs are seen clearly. Through detail simulations, the heat transfer modes, flow pattern, and its distribution within combustion zone have been analysed to enable understanding of the heat release rate. The CFD simulation plotted results, heat release rate and radiation distributions and total heat transfer in boundary zone are visualized in the flowing figures.

4.1.1 Heat release rate

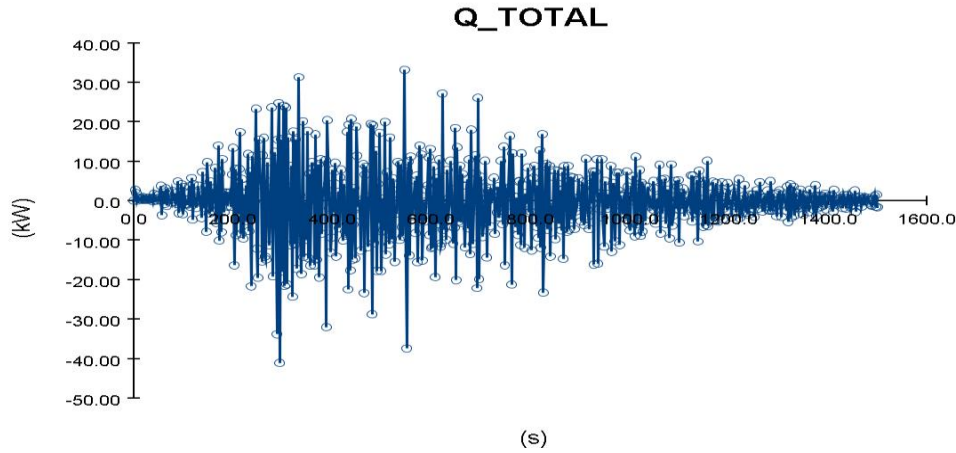
The heat release rate curve from waste combustion fire inside the model zone is shown the figure 04. It is seen that during the combustion the heat release is varied with time because of various factors (environmental conditions, nature of combustible materials etc.). It is observed that first 3 minutes of ignition the HRR increases to reach at maximum point (1000 KW) between 3 to 4 minutes after the combustion, then it decreased until the combustion of waste sample is ended.



Graph 4. CFD simulation result, heat release rate of combustion

4.1.2 Total heat transfer

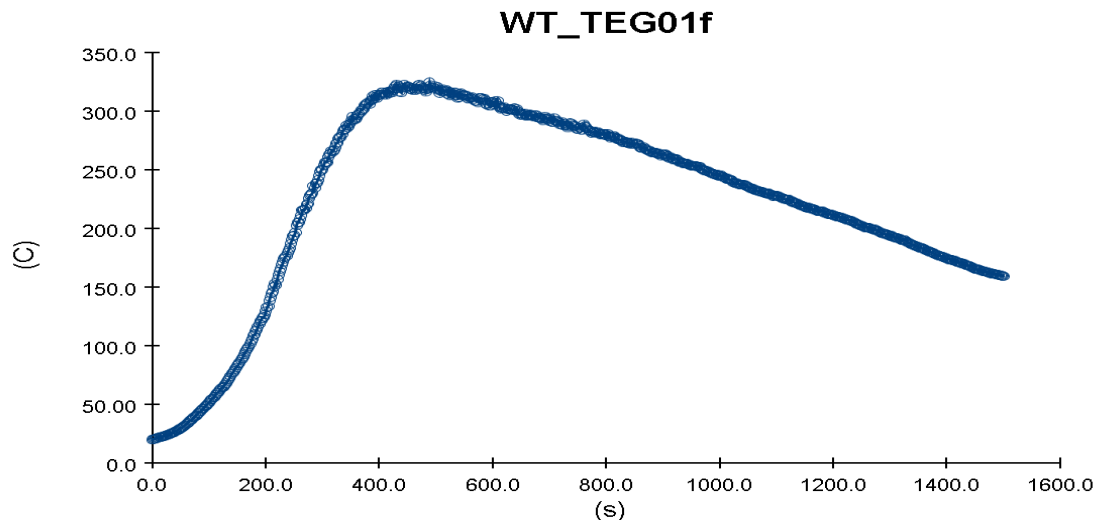
The total heat with time from combustion is given following figure. It is seen between first 3 to 7 minutes the total heat is at peak point, with time it decreases due to reducing of combustion reaction. The simulation time 25 minutes is noted until is ended of sample combustion with zero total heat.



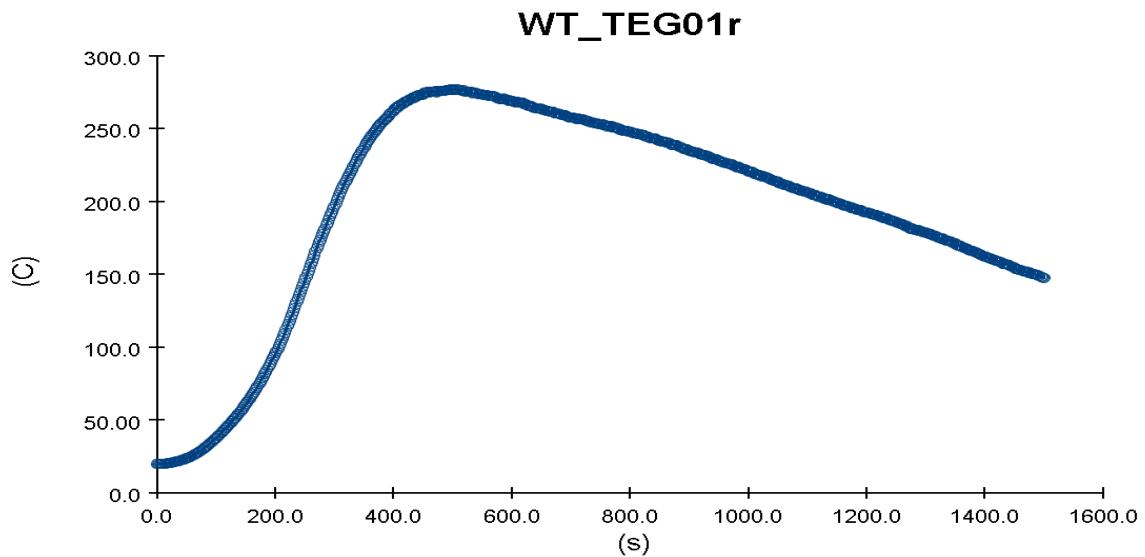
Graph 5. CFD simulation result, total heat transfer from combustion.

4.1.3 Temperature across the TEGs

The following temperature curves show the front and back temperature of TEG 01 respectively. The temperature on both side is raising in first 7 minutes of combustion, then it is decreased until the end of simulation time (25 minutes). The front side of TEG face the fire, having higher temperature, the maximum temperature about 320 C is noted after 7 minutes of ignition. Similarly, the temperature at colder sider of TEG is increasing in first 7 minutes and reaches approximately 280 C. At the same way, temperature curves for all 32 TEGs have been determined as for this research. However, this report contains faces temperature curves of only TEG 01. The all TEGs have the similar temperature cavers but having different temperature values to TEG 01.



Graph 6. the temperature at front side of TEG 01.



Graph 7. the temperature at colder side of TEG 01.

From the CFD simulation, the temperature at hot and cold sides of TEGs is noted for analysing the power generation. The heat release rate from fire sources and temperature difference between TEGs are the most useful outcome of FDS simulation further calculating the TEGs power generation. There were 12 different scenarios (discussed above in the previous chapter 03) are made for this study, the simulation of individual cases is done by CFD.

4.2 Power Generation from TEGs

After a carefully assessment the useful variables, heat release rate and temperature differences across the TEGs enable to analysis the power generation of TEGs from different type of waste combustion with different scenarios.

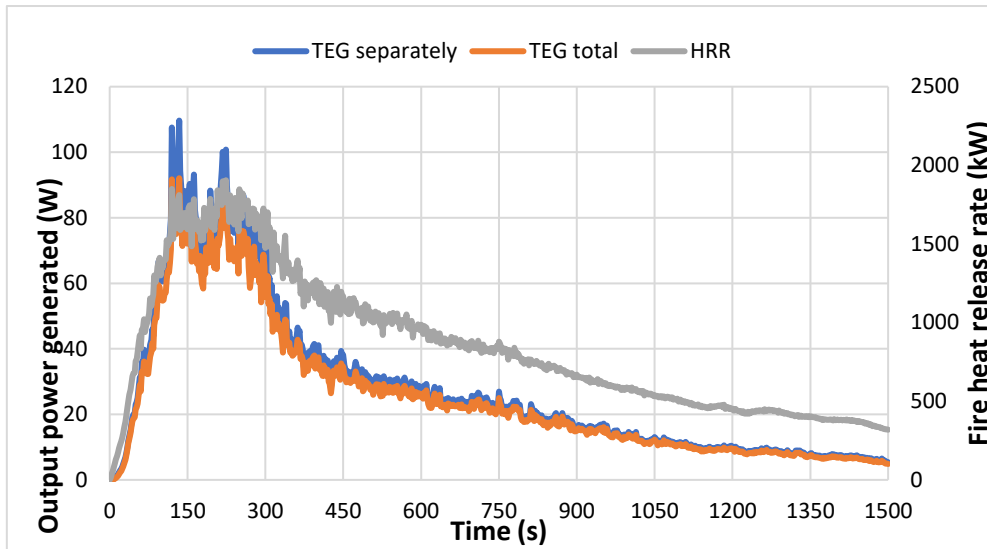
4.2.1 Generated Power from wood pellets fire Scenarios

There were four scenarios made of wood pellets as the heat source of TEGs. The cases were run by the FDS to assess the heat release rate. That effect is the final output generated power.

The final outcomes of scenarios: The total generated power from TEGs (all connected in series) is given the following graphs. Output power of series connected TEGs and separated TEGs depends on the heat release rate from the waste burning which is different in following scenarios.

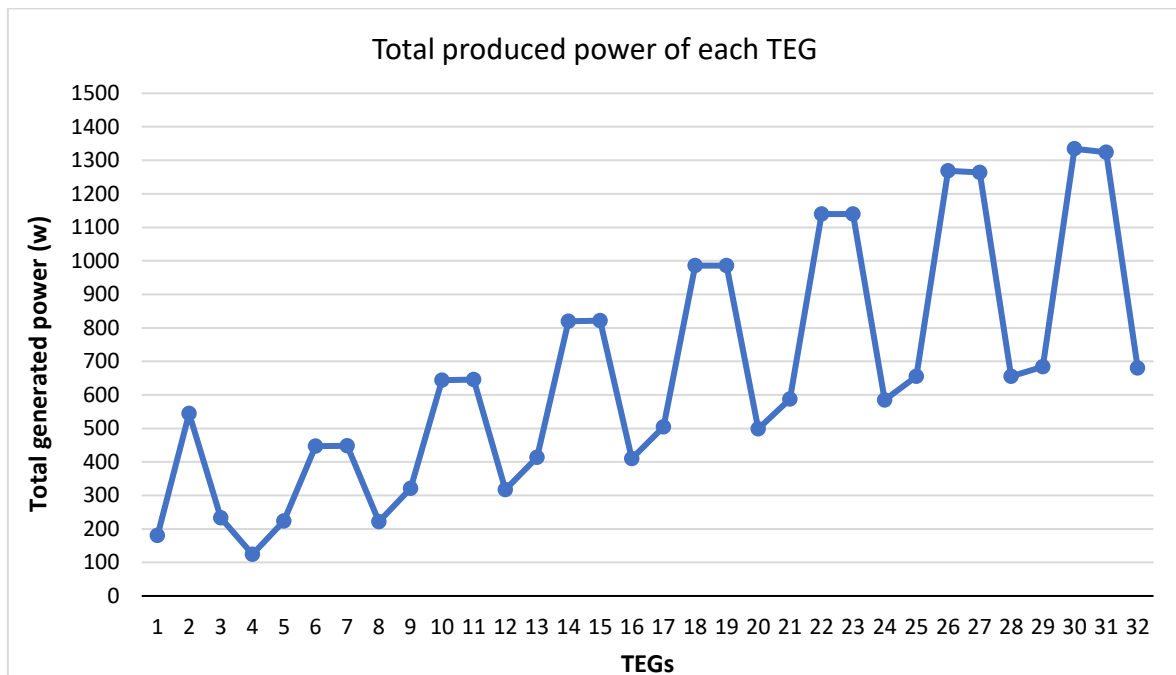
1. TEGs without heatsink and with no lateral wind.

The heat release rate and power quality of TEGs with absence of heatsink and lateral wind from wood pellets waste combustion is shown in graph 04. The combustion test was completed in 25 minutes. It is observed that in first 2.5 minutes of ignition the TEGs generated power and heat release are at peak. At this point maximum power 110 W is noted for individual TEGs and for their series connection peak power is 90 W. The power decreases when TEGs are connected in series due to cable losses. It is cleared that HRR from waste combustion strongly effects the output power of TEGs. It is shown in the following graph after two or three minutes of ignition HRR is decreasing it causes to reduce the total output power of TEGs.



Graph 8. the generated output power of TEGs and heat release rate from wood pellets waste combustion without heatsink and with no lateral wind.

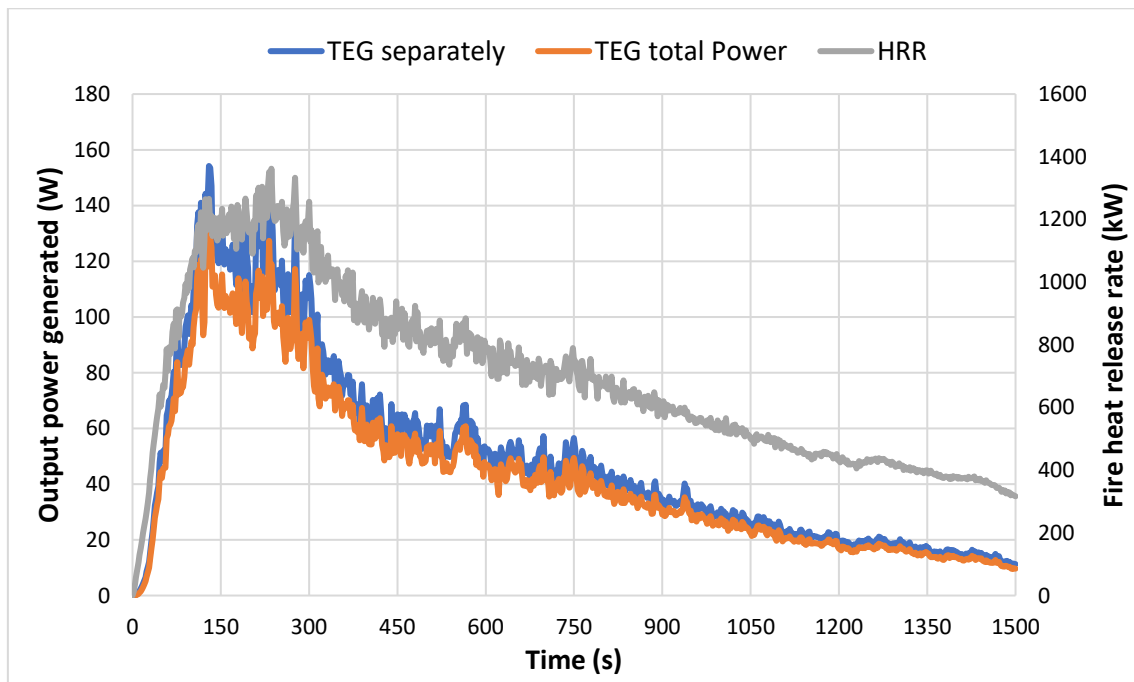
The total power production of each TEG is varied. TEG 30 is generated higher output power (approximately 1330 W) as shown in the graph 05. With compared to other TEGs, TEG 4 produces least power with wood pellets combination source in this scenario. In Actual this is because of temperature gradient across the TEGs. Thus, the temperature gradient depends on the TEGs' faces temperature, it relies on the position of TEG on the sheet. Some TEGs, including TEG 4 are received lowest heat release rate from fire source compared to TEG 30. Hence, their power production is observed lower.



Graph 9. total generated output power of TEGs with wood pellets waste combustion.

2. TEGs without heatsink and with lateral wind.

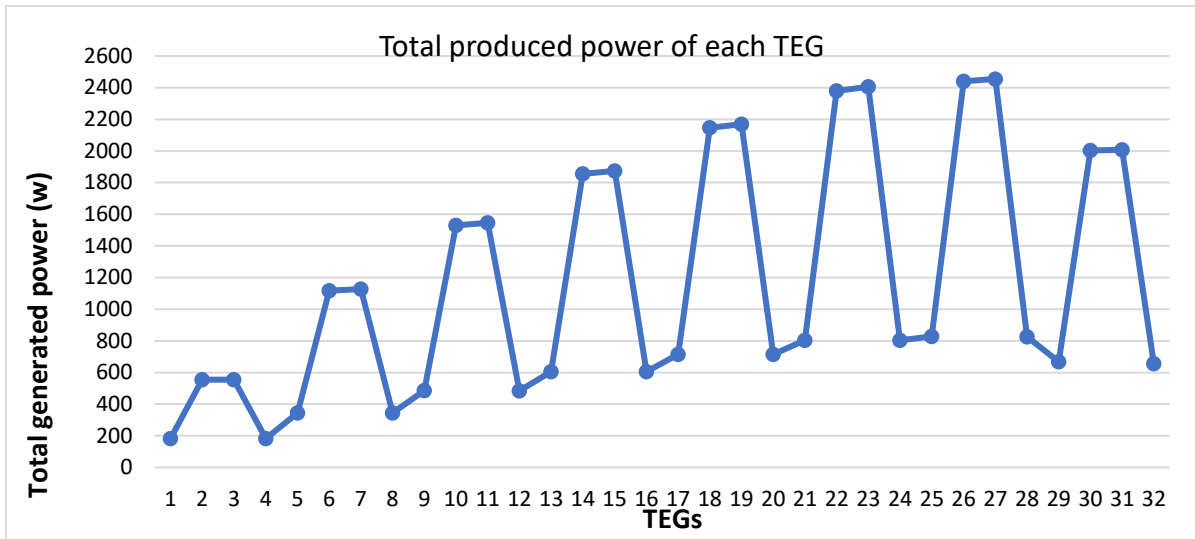
The scenario TEGs with lateral wind increases the heat release rate from wood pellets is indicated in the following graph 06. The optimal output power (130 W) of the system is achieved after 3 minutes of ignition. It is observed that the lateral wind is nicely improved the TEGs output power. It increases the TEGs total power individually as well as output power with their series connection. The lateral wind leads to a great combustion of waste to maximize the heat release rate then it causes to increase the temperature difference between TEGs faces and finally it increases overall output power of TEGs. The total heat release rate with TEGs total output power is noted in 25 minutes, is taken time of waste combustion. At first three minutes higher flam is provoked to sudden rising of hate release rate and then it decreases gradually after 3 minutes till to completed burn of waste in 25 minutes.



Graph 10. the generated output power of TEGs and heat release rate from wood pellets waste combustion without heatsink and with lateral wind.

The total power production of each TEG without heatsinks and with lateral wind from wood pellets fire is given in graph 07. The maximum total output power is 2455 W which is produced by TEG 27. The minimum power is 180 W which is generated by TEGs 1 and 4. It is cleared that lateral wind reduces the temperature at cold face to increase the overall power of TEGs. Mostly this scenario improves the power generation quality in

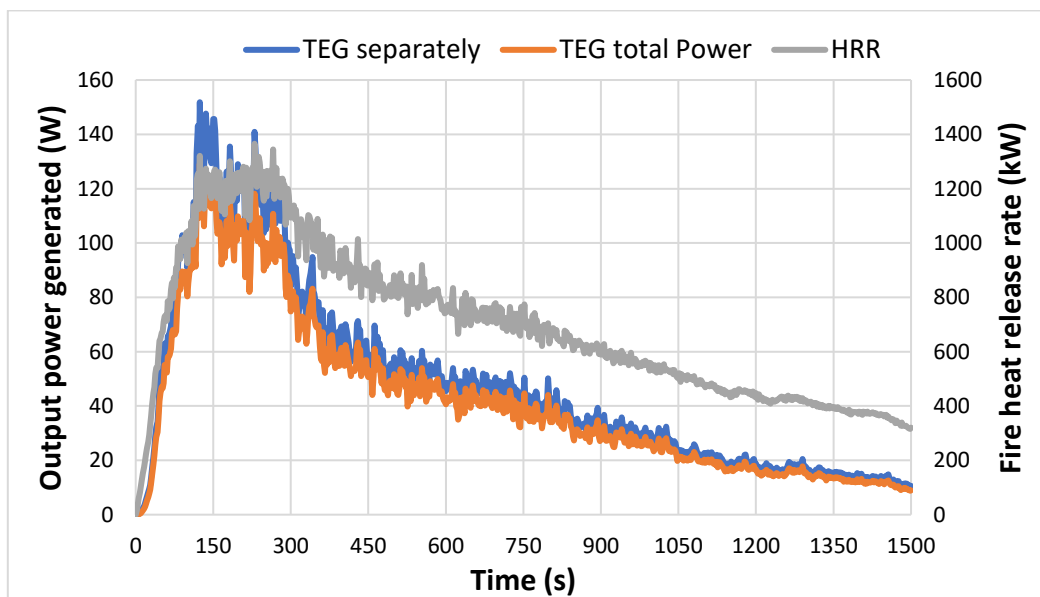
TEGs 27 and 26 due to get higher temperature difference because of receiving more heat at hot side.



Graph 11. total generated output power of TEGs with wood pellets waste combustion without heatsink and with lateral wind.

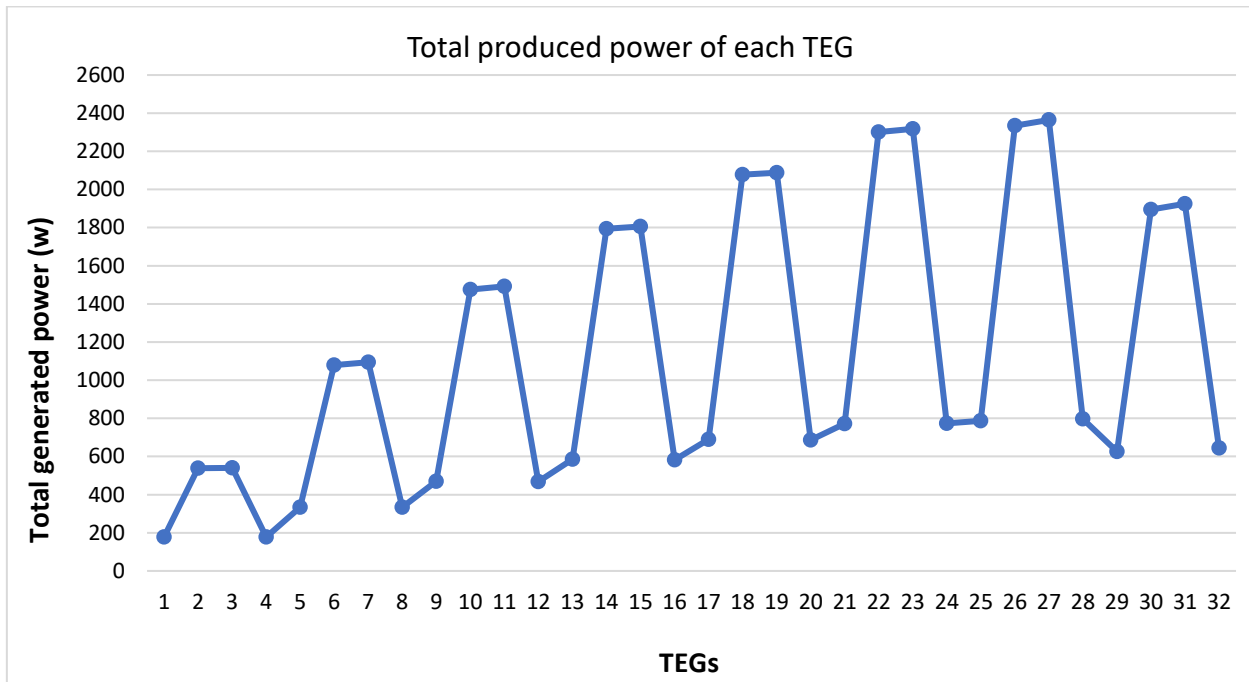
3. TEGs with heatsink and with no lateral wind.

Like TEGs with lateral wind scenario, the maximum heat release rate (1300 kW) after 3 minutes of agitation is noted in TEGs with heatsink scenario is shown the graph 08. At the same point TEGs have peak total output power with series combinedly or separately. The TEGs with heatsink produce overall same



Graph 12. the generated output power of TEGs and heat release rate from wood pellets waste combustion with heatsink and with no lateral wind.

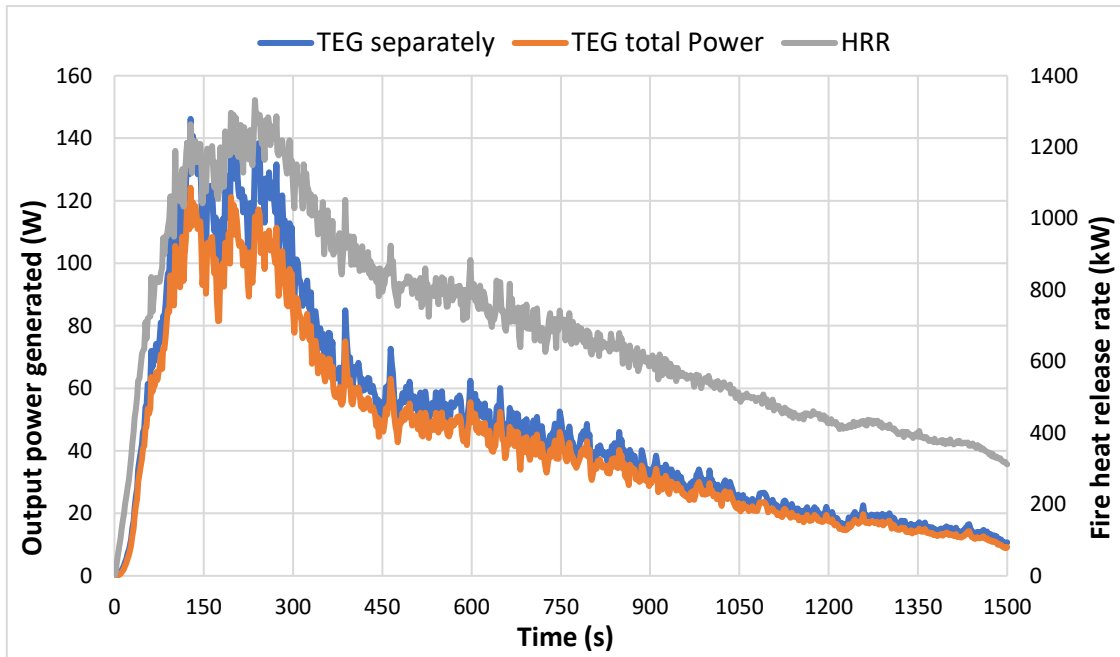
The total power quality of each TEG with heatsink scenario from wood pellets combustion is shown in the following graph 09. Like the previous scenario the higher output power generation approximately 2300 W is noticed in TEG 27 and the minimum power is produced by TEG 4. like lateral wind, heatsink also reduces the temperature at cold side of TEG to improve the overall power of TEGs.



Graph 13. total generated output power of TEGs with wood pellets waste combustion.

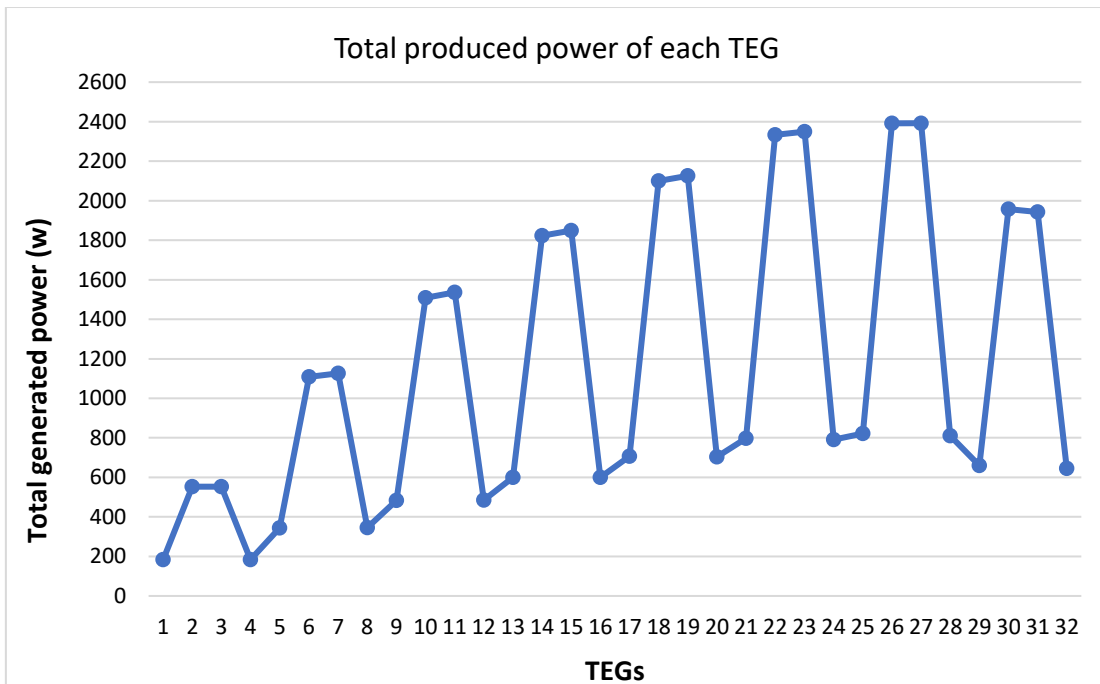
4. TEGs with heatsink and with lateral wind.

The generated power from TEGs with heatsink and with lateral scenario is shown in the graph 10. TEGs with both, heatsink and lateral wind does have the same effect on power quantity as TEGs with each of them. It is shown in following graph after 5 minutes ignition the HRR and TEGs generated power is gradually decrease until finish the combustion in 25 minutes. In this scenario the maximum heat release 1300 kW is observed with peak TEGs output power 130 W. A big difference between heat release rate and electric power is noticed because of low energy conversion efficiency of TEGs devices.



Graph 14. the generated output power of TEGs and heat release rate from wood pellets waste combustion with heatsink and with lateral wind.

The graph 11, shows total generated power of each TEG with heatsink and with lateral wind from wood pellets burning. In this scenario it is observed that TEG 27 and 26 are produced max output power (about 2390 W). The lowest output power is produced by TEG 4 and 1 like previous scenarios. Therefore, TEGs performance with heatsink and with lateral wind is almost similar to TEGs with heatsink or TEGs with lateral wind.



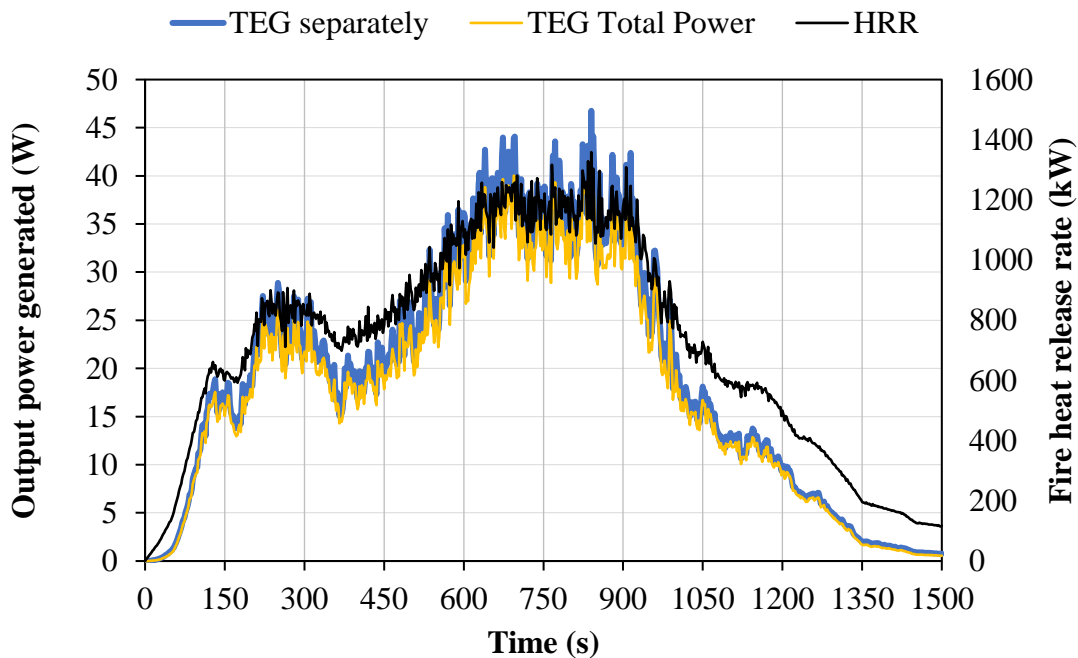
Graph 15. total generated output power of TEGs with wood pellets waste combustion.

4.2.2 Generated Power from rubber and trash can fire Scenarios.

Rubber and trash can waste are used to burn as heat source for power generation through TEGs in four different scenarios, discussed below. The output generated power depends on heat release rate from waste fire.

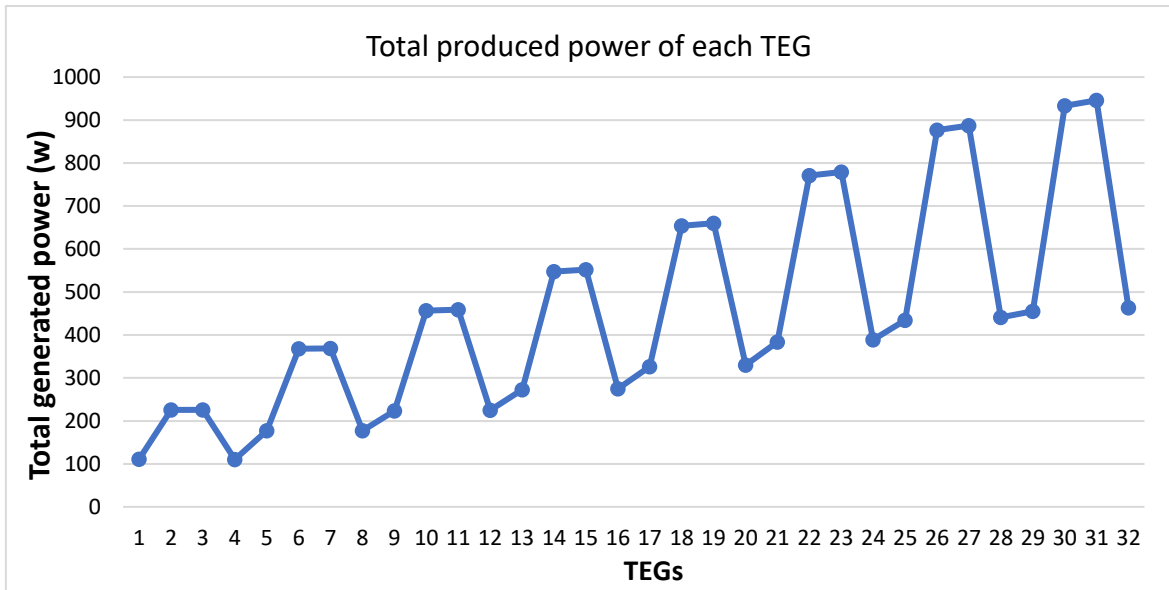
1. TEGs without heatsink and with no lateral wind.

The total heat release rate of TEGs with no heatsink and no lateral wind from rubber and trash cans fire is given in the graph 12. Unlike wood pallets waste burning, rubber and trash cans combustion produce maximum power (38 W) with at peak heat release rate 1490 kW by eleven minutes of ignition. This type of waste has a good combustion in a wide range of time to maintain the quality of heat release rate.



Graph 16. generated output power of TEGs and heat release rate from rubber and trash can waste combustion without heatsink and with no lateral wind.

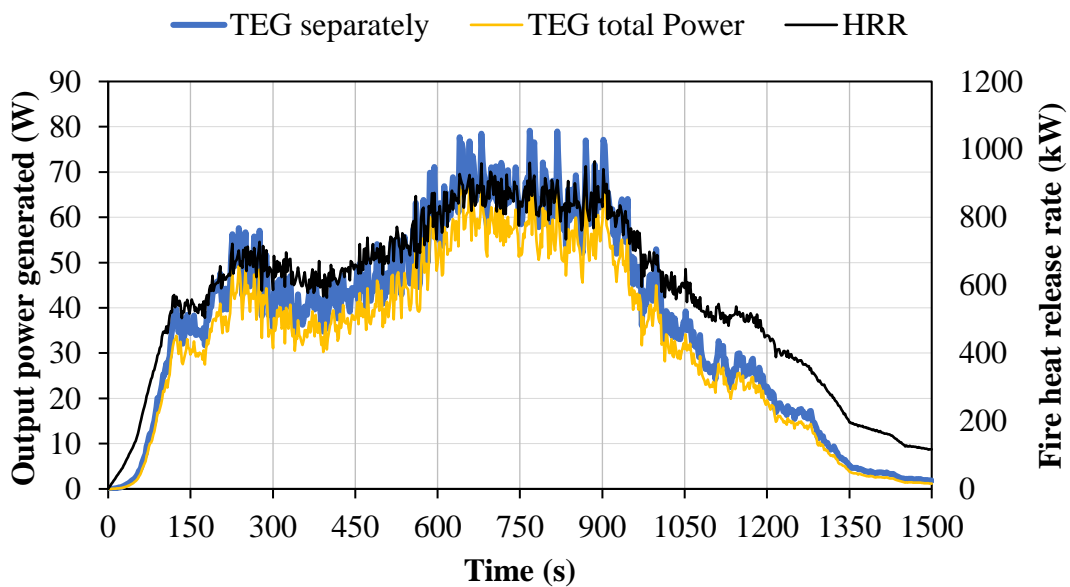
The total power generation of TEGs without heatsink and without lateral wind from rubber and trash cans combustion is given in the graph 13. The TEG 31 and 30 are produced peak output power which are about 950 W and 940 W respectively. The minimum power is approximately 100W which is generated by TEGs 1 and 4. The TEGs receive higher heat rate from the fire produce more power because of having higher temperature different.



Graph 17. total generated output power of TEGs with rubber and trash cans waste combustion without heatsink and with no lateral wind.

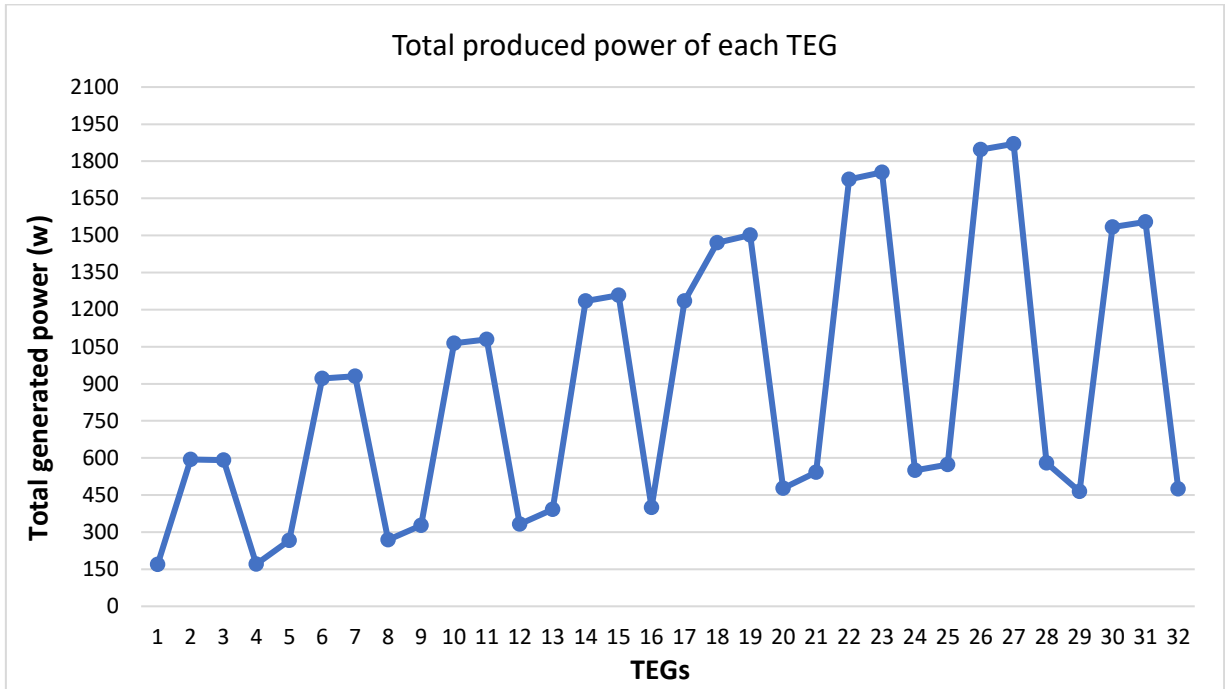
2. TEGs without heatsink and with lateral wind.

The scenario, TEGs with lateral wind and without heatsink increases the heat release rate is indicated in the following graph. The maximum generated power 60 W of series connected TEGs with 1090 kW HRR is achieved after 10 minutes of ignition. The average output power of TEGs (separately and series connected) increases when considering the effect of lateral wind.



Graph 18. generated output power of TEGs and heat release rate from rubber and trash can waste combustion without heatsink and with lateral wind.

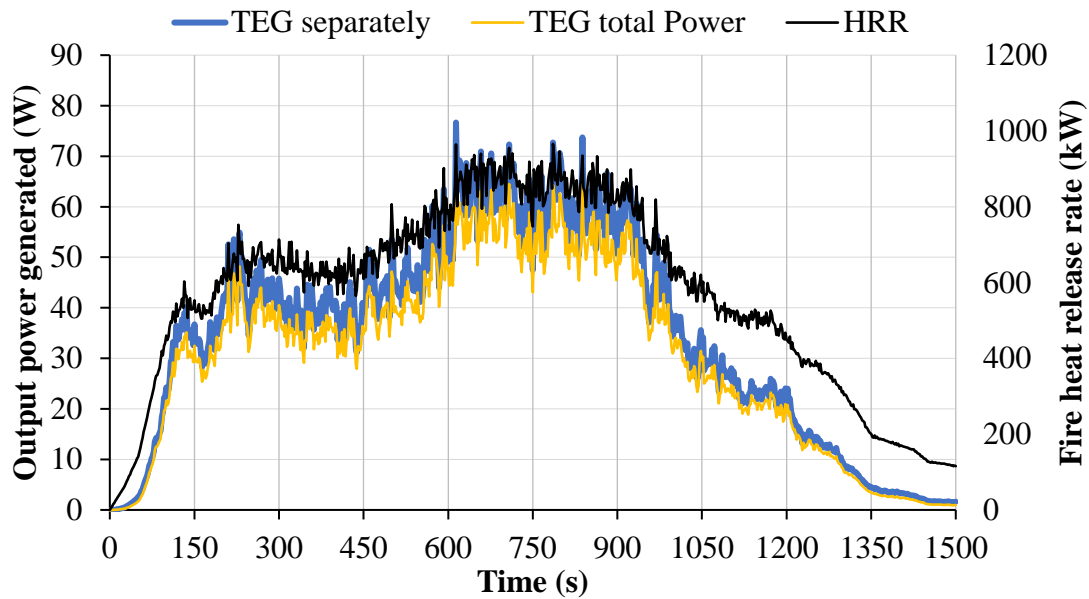
The following graph 15 describes the total output power of TEGs with lateral wind and without heatsink from rubber and trash cans fire is given in the graph 15. In this scenario TEG 27 and 26 are produced higher power, 1870 W and 1840 W respectively. TEGs 1 and 4 are generated lowest power about 150 W each. Thanks to lateral wind for increasing temperature difference across the TEGs to increase the final output power.



Graph 19. total generated output power of TEGs with rubber and trash cans waste combustion without heatsink and with lateral wind.

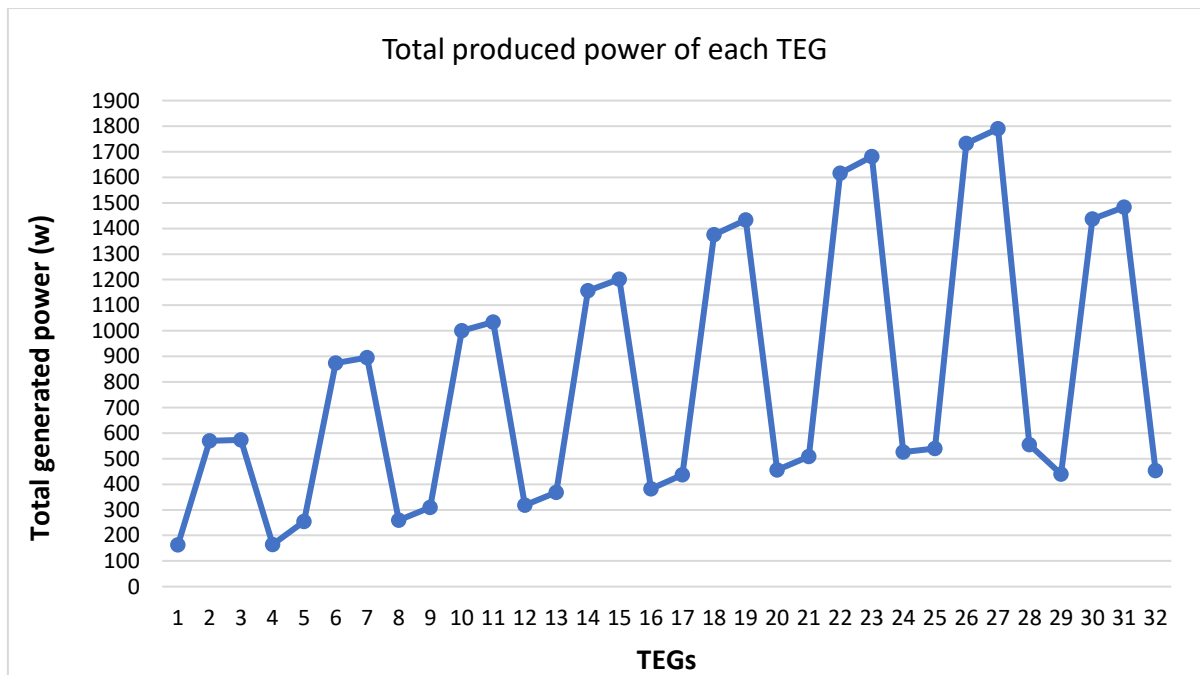
3. TEGs with heatsink and with no lateral wind.

The heat release rate from rubber and trash cans combustion and output power of TEGs with heatsink and without lateral wind is mentioned in the graph 16. It is cleared in following figure peak heat release rate 1000 kW is released after eleven minutes. At the same point the output power of TEGs, separately (65 W) and series connected (70 W) is noticed maximum. The TEGs having heatsink have much similar results to TEGs with lateral wind. In both cases, the improvement in heat release rate is observed due to have lateral wind and heatsink. Finally higher power is achieved to have lateral wind or heatsink in TEGs system.



Graph 20. generated output power of and with heat release rate from rubber and trash can waste combustion with heatsink and without lateral wind.

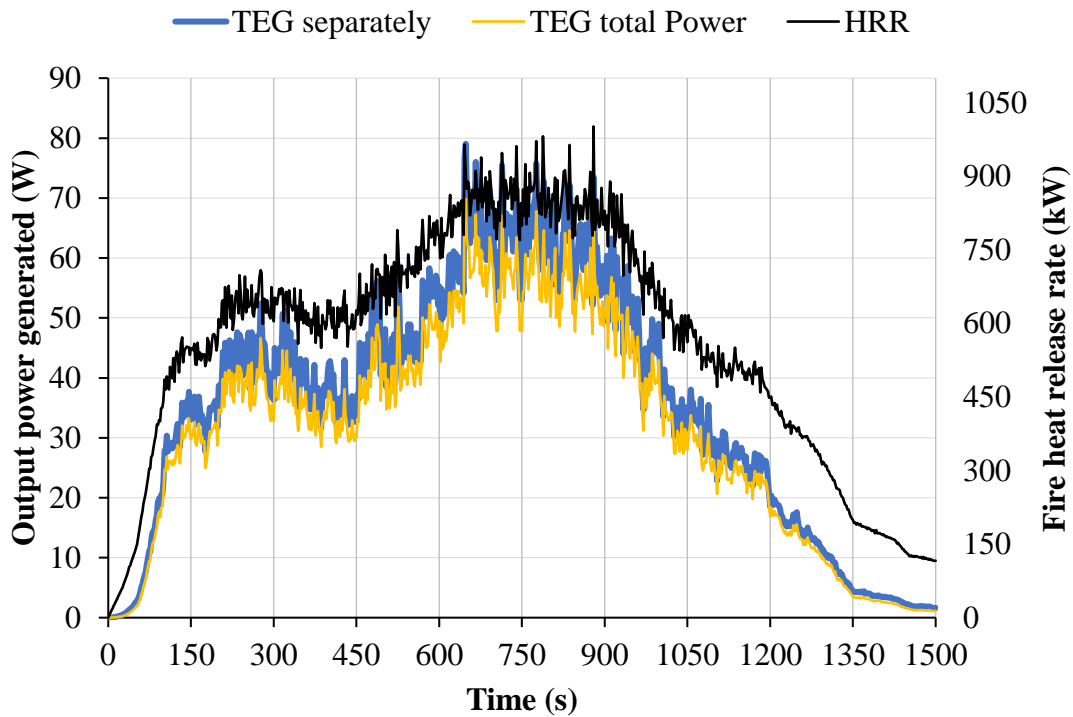
The total power generation of TEGs with heatsink from rubber and trash cans combustion is given in the graph 17. The total maximum power is 1790 W, produced by TEGs 27 and minimum power is 165 W, produced by TEG 4. Hence, the heatsink also improves the performance of TEGs. It helps to receive higher heat from the fire source to make a good temperature different.



Graph 21. total generated output power of TEGs with rubber and trash cans waste combustion with heatsink and with no lateral wind.

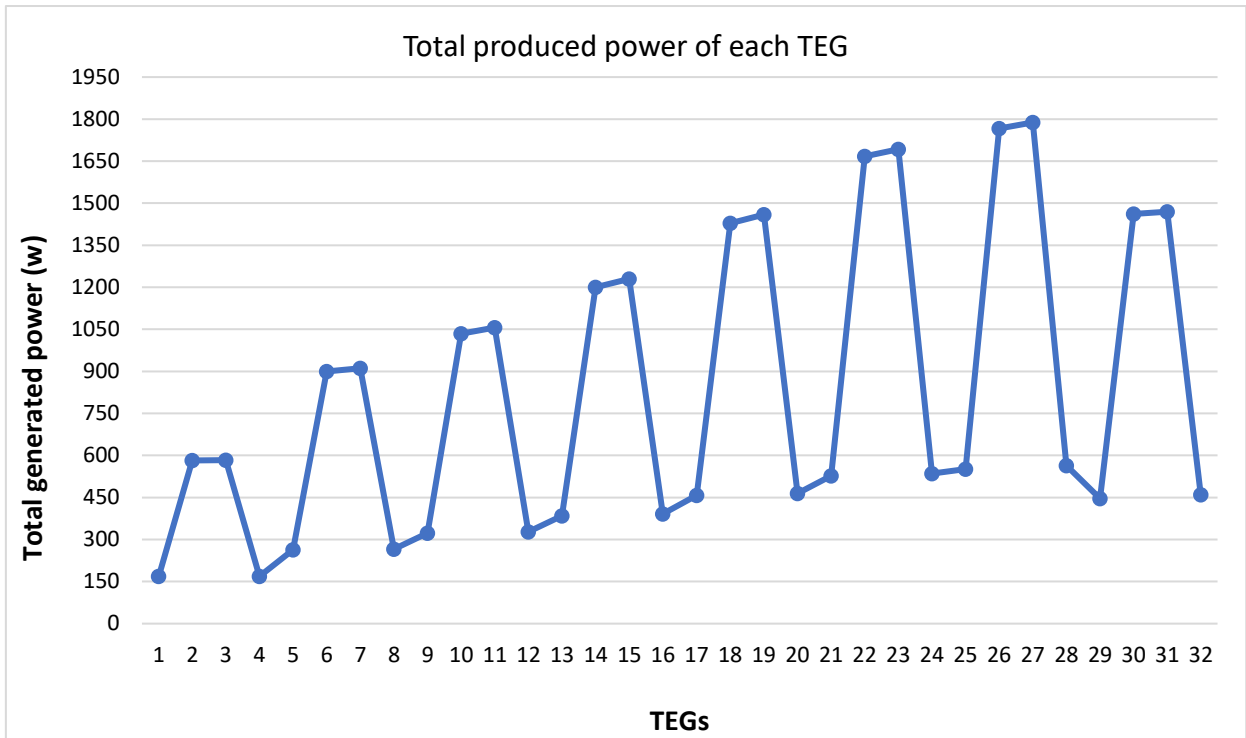
4. TEGs with heatsink and with lateral wind.

The below graph describes the output power of TEGs with heatsink and lateral wind and heat release rate of rubber and trash cane combustion. In this scenario is higher heat release rate 1000 kW with peak power 80 W of each TEG is noticed at 15 minutes of combustion. A fluctuation is seen in HHR before its' peak point between 5 and 6 minutes in combustion duration.



Graph 22. generated output power of TEGs and with heat release rate from rubber and trash can waste combustion with heatsink and with lateral wind.

In the following graph 19, it shows the TEGs with heatsink and with lateral wind as same maximum and minimum generated power is TEGs with heatsink from rubber and trash cane combustion. It is also seen that same TEGs have similar power values in both cases. Having both, heatsink and lateral does not change the output power of TEGs, even their individual presence is more effective than combined used.



Graph 23. total generated output power of TEGs with rubber and trash cans waste combustion with heatsink and with lateral wind.

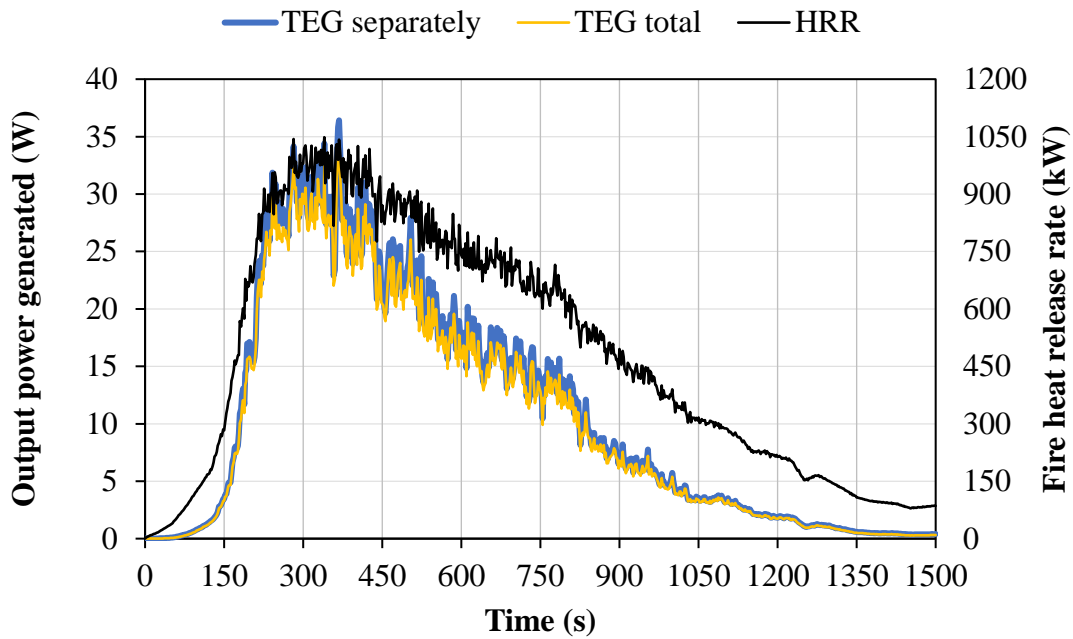
4.2.3 Generated Power from cardboard boxes fire

Power generation from burning of cardboard boxes filled with polystyrene cups wastes through TEGs in four different scenarios are following.

1. TEGs without heatsink and with no lateral wind.

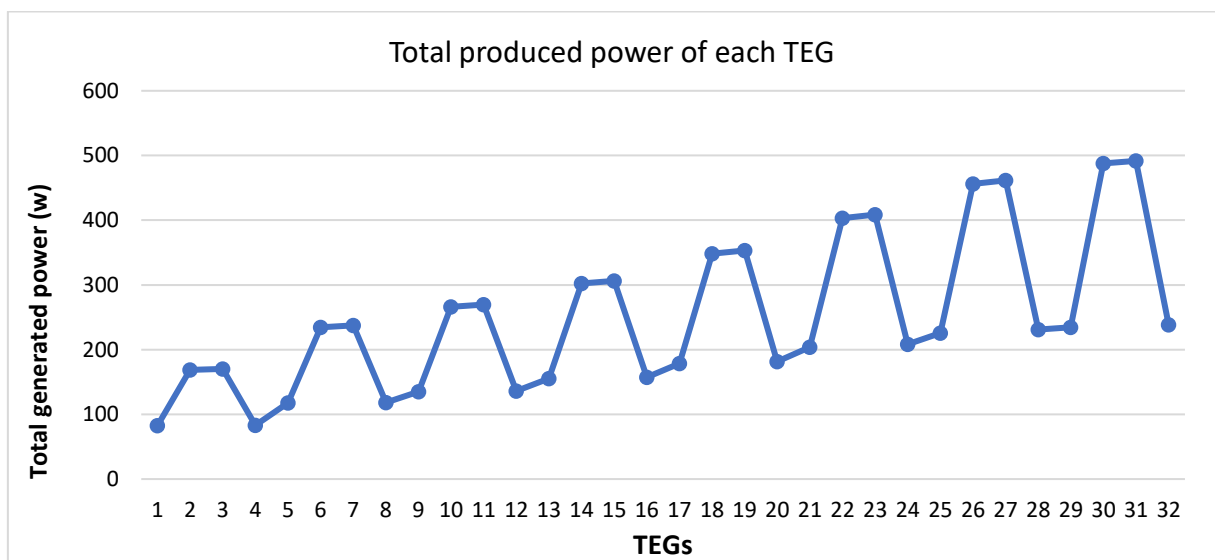
The heat release rate and TEGs generation power without heat sink and with no lateral wind from cardboard boxes waste fire flam are given in graph 20. It is observed that maximum heat release rate 1020 kW is released in 6 minutes of ignition. At this point higher power 35 kW is generated from TEGs (series connected) and similarly 30 W higher power is generated by TEG separately.

Except the values, combustion and heat release rate scenario of cardboard boxes are quite same to wood pellets combustion and heat release rate. The HHR is much lower in the cardboard combustion than HHR in wood pellets combustion.



Graph 24. generated output power of TEGs and heat release rate from cardboard boxes waste combustion without heatsink and with no lateral wind.

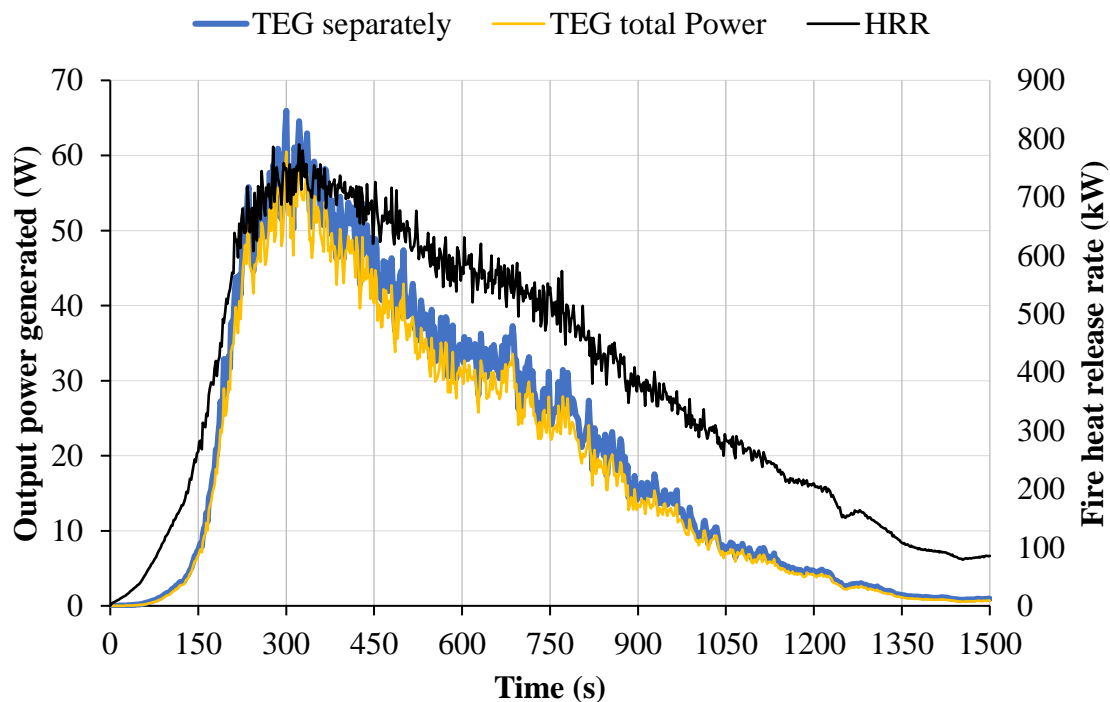
The individual TEG without heatsink and without lateral wind total power generation from cardboard boxes combustion is mentioned in following graph 21. It is shown that TEG 30 and 31 produce higher power 492 W and 496 W respectively. Like earlier discussed scenarios, TEG 4 is produced lower power in this case. Overall generated power of each TEG from cardboard boxes burning is less than wood pellets and trash cans combustion. It is due to lower heat release rate is shown in above graph 20, leads to get lower temperature gradient across the TEGs.



Graph 25. total generated output power of TEGs with cardboard boxes waste combustion

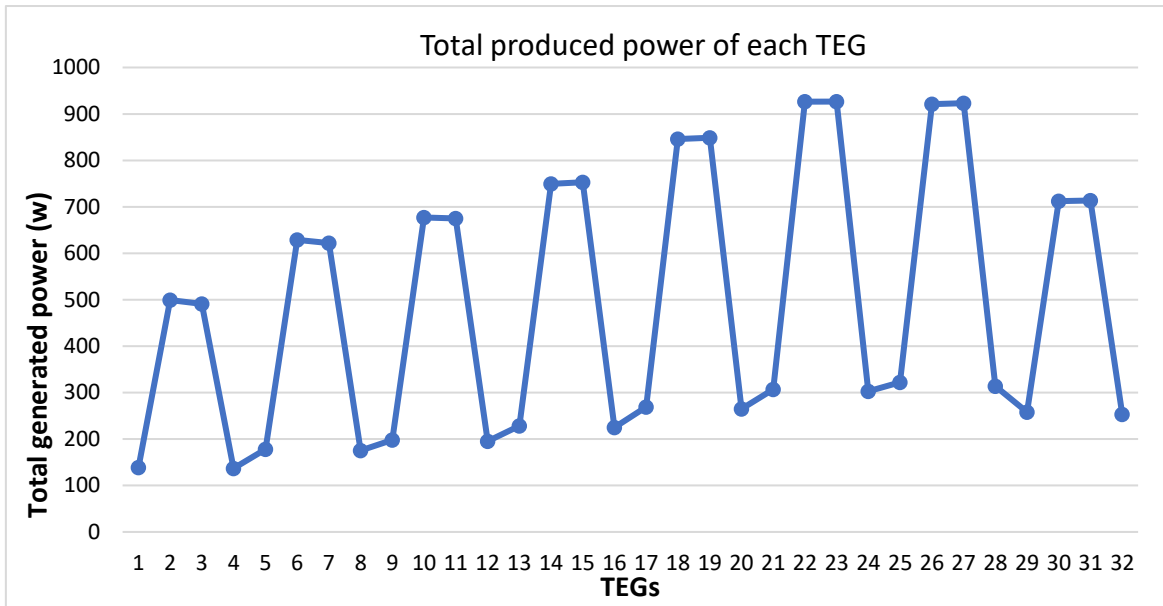
2. TEGs without heatsink and with lateral wind.

The results of TEGs with lateral wind and without heatsink scenario are shown in the graph 22. The peak HRR 800 kW is released with generated 65 W optimal output power from series connected TEGs after 5 minutes from ignition starting. It is observed that the lateral wind increases 50% the TEGs output power. The TEG separately maximum power 58 W is gained at peak point of heat release rate. It is seen that lateral wind provoke a good combustion of waste to maximize the heat release rate then it causes to increase output power of TEGs. The waste combustion time 25 minutes are taken for every type of combustion with all scenarios. Like wood pellets combustion at few minutes the peak flam is observed to rise the hate release rate and then it decreases gradually after 5 minutes till to completed burn of waste in 25 minutes.



Graph 26. generated output power of TEGs and heat release rate from cardboard boxes waste combustion without heatsink and with lateral wind.

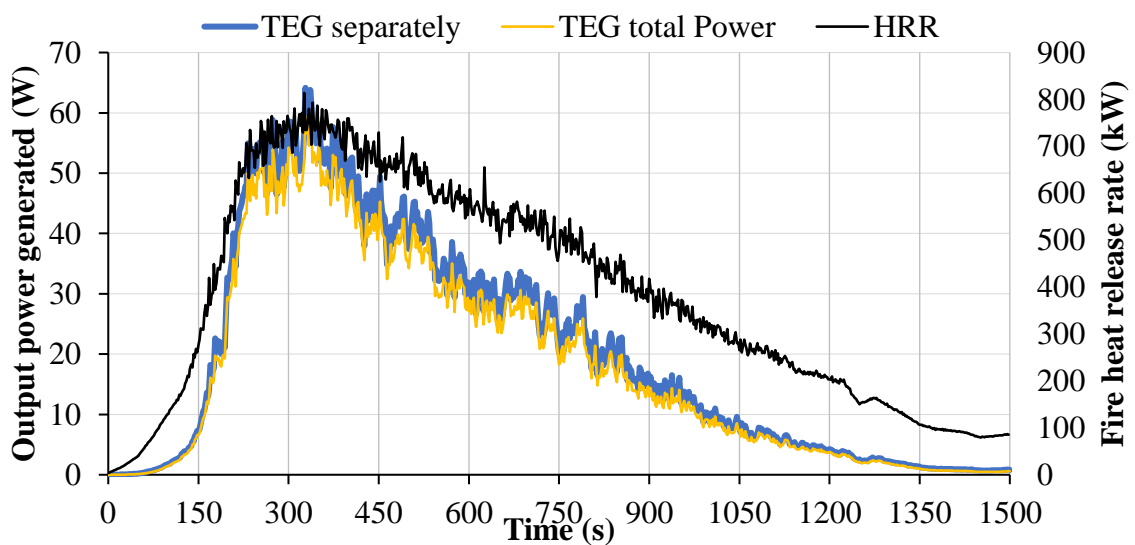
The total generated power from TEGs with lateral wind total power from cardboard boxes combustion is shown in following graph 23. In this scenario higher generated power is noted 926 W by TEG 22 and 23 each. The minimum generated power produced by TEG 4 with producing 137 W. It is happened due to increase of heat release by having lateral wind.



Graph 27. total generated output power of TEGs with cardboard boxes waste combustion.

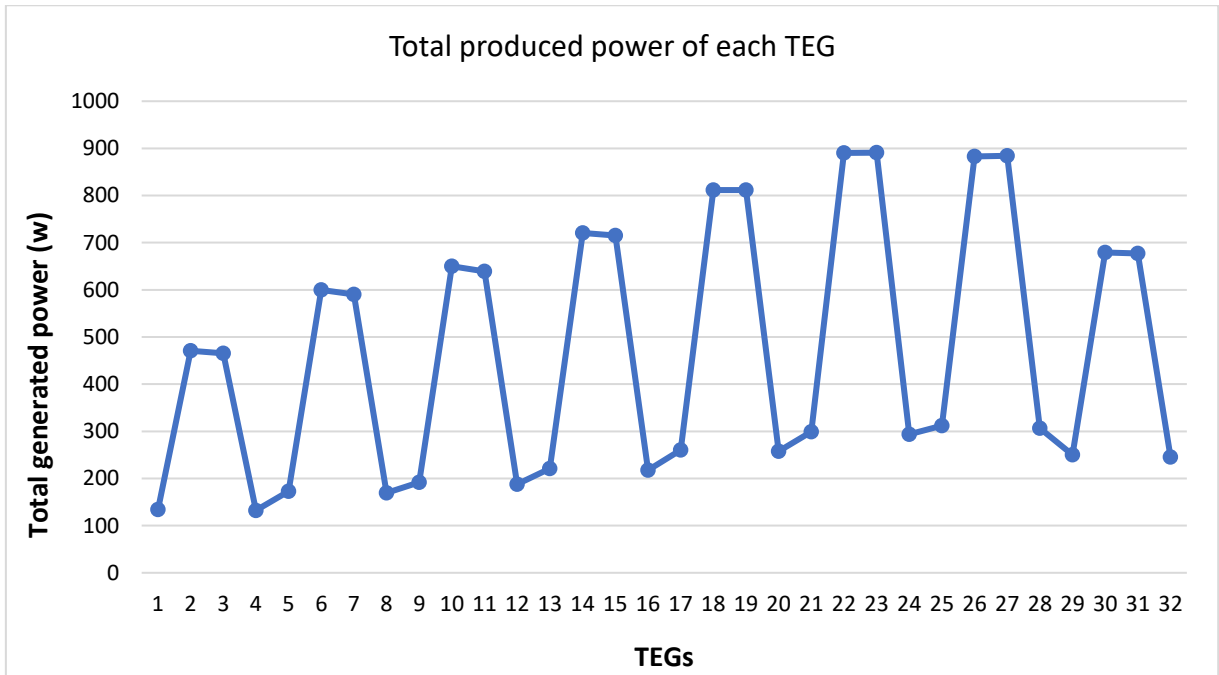
3. TEGs with heatsink and with no lateral wind.

The heat release rate and power from TEGs with heatsink and without lateral wind are given in the graph 24. It can be seen from graph having heatsink in TEGs system has the almost similar effect on heat release rate as TEGs with lateral wind has. In this scenario, maximum heat release rate 800 kW and TEGs (series connected) total power 55 W are observed after 5.5 minutes of combustion. The maximum 64 W TEG separately power generation is noted from this kind of waste combustion.



Graph 28. generated output power of TEGs and heat release rate from cardboard boxes waste combustion with heatsink and with no lateral wind.

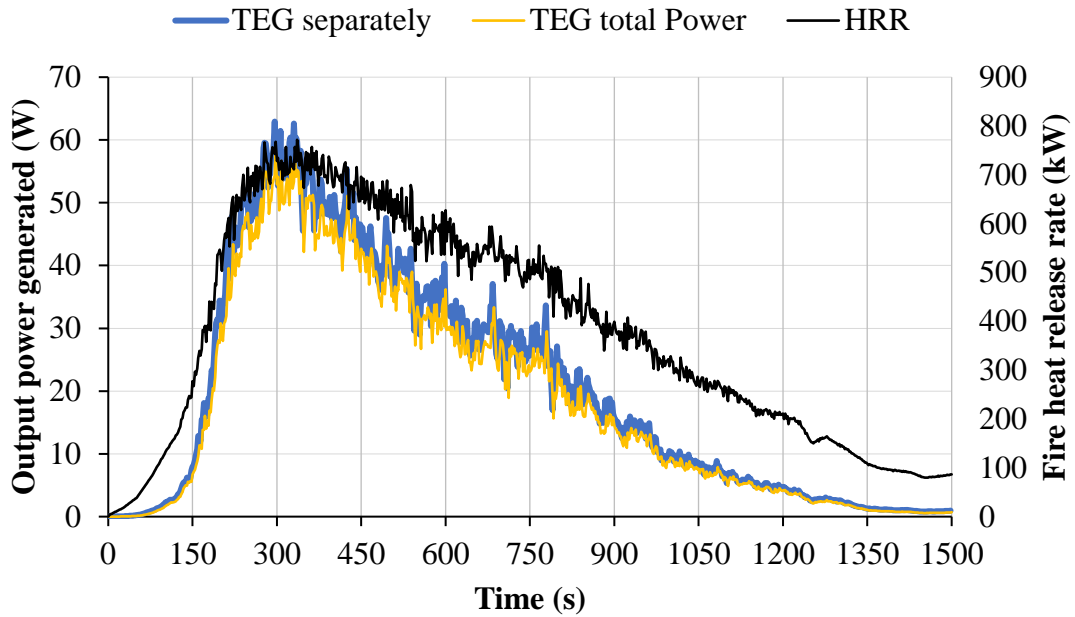
The following graph 25 describes the total generated power from TEGs with heatsink from cardboard boxes combustion. In this scenario higher generated power 890 W is observed by TEG 22 and 23 each. The minimum generated power 132 W is produced by TEG 4. Mostly TEGs with heatsink as same results as TEGs with lateral wind.



Graph 29. total generated output power of TEGs with cardboard boxes waste combustion.

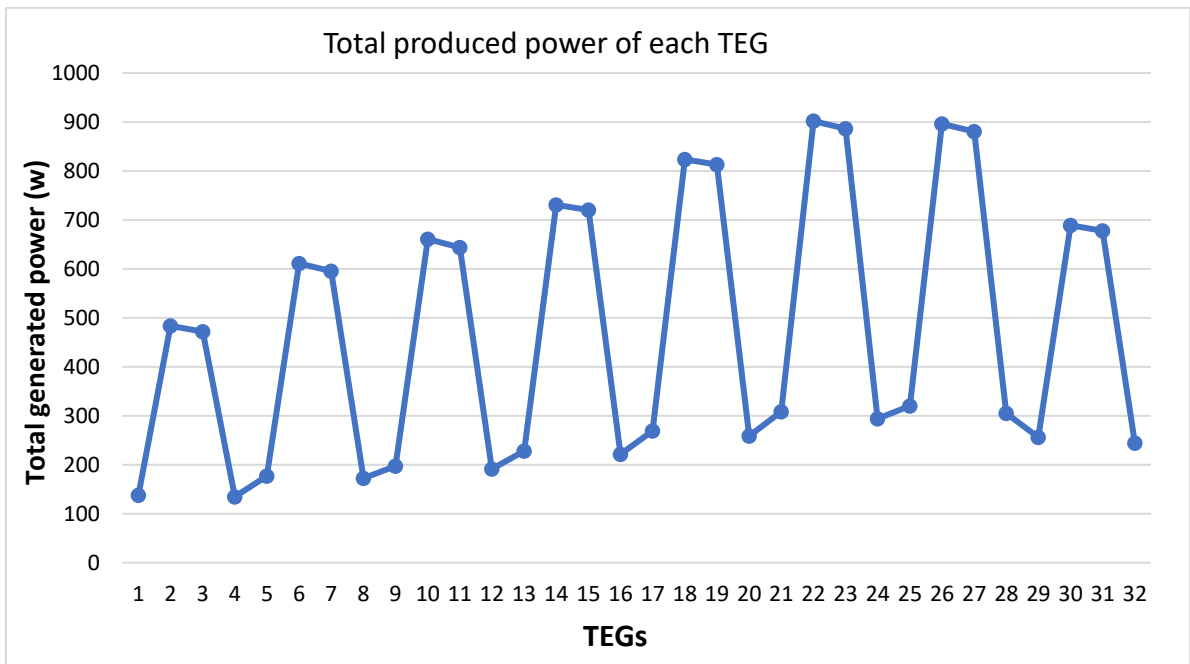
4. TEGs with heatsink and with lateral wind.

The graph 26 shows the heat release rate and output power of TEGs with heatsink and lateral wind. After 5 minutes of the waste combustion maximum heart release rate 780 kW is noted. At the same point TEG total generated power (55 W) and individually TEG generated power (62 W) is observed. Considering both, heatsink and lateral wind for TEG does not impact on the heat release rate from flam. This scenario (TEGs with heat sink and with lateral wind) has almost the same results as previous scenario (TEGs with only lateral wind).



Graph 30. the generated output power of TEGs and heat release rate from cardboard boxes waste combustion with heatsink and with lateral wind.

TEGs having both, heatsink and lateral wind with cardboard boxes fire is maximized the total outpower to 902 W of TEG 22 is shown in the graph 27. In this scenario lower generated power 135 W is observed by TEG 4. Like other types of waste burning, cardboard boxes combustion with TEGs heatsink and lateral wind have similar results.



Graph 31. total generated output power of TEGs with cardboard boxes waste combustion.

4.3 Conclusion

In conclusion, this study has presented a comprehensive investigation of the CFD analysis of thermal energy harvesting from waste combustion as heat source. The primary objective of this thesis is the generating of electric energy by utilizing TEGs from a waste fire as a sustainable sources of thermal energy.

By using the CFD techniques, this research has provided valuable insights into the thermal behaviour of waste fire and its interaction with TEGs. Through detail simulations, the heat transfer mechanism, flow pattern, and temperature distribution within combustion zone have been analysed, enabling a comprehensive understanding of the thermal energy conversion process.

As the study is mainly focused on three types of waste for combustions: wood pellets, rubber and trash can, and cardboard boxes. The selection of waste types was done after a detailed review of literature on the bases of their availability, high heating value, and easier to manage. Some important data like total heat release rate, peak heat release rate after agitation time, and total taken time of combustion of waste samples are collected from the National Fire Laboratory. Based on waste combustion information, the CFD analysis is made with the design parameters, such as sandwich materials form of thermocouple, heat exchanger configuration, and operating conditions. The different types of waste combustion conditions with TEGs were simulated in the CFD fire code. The potential of TEGs as an efficient means of converting the harvested thermal energy from the waste into electric energy was noted in the results of CFD simulation.

Moreover, in this work there are four different scenarios of operation conditions are made for TEGs system about heatsink and lateral wind for each type of waste burning. The output power generation of the 32 TGEs devices for each scenario is observed after temperature difference assessment through the CFD simulation. As it is seen in the results that heat release rate and temperature differences have a strong impact on the output power of the system. It is perceived that after the calculation of total power of TEGs for each type of waste, the total power generation of TEGs with wood pellets fire is observed higher than other to types of waste (rubber and trash cans, and cardboard boxes). Hence, the total power generation of TEGs with rubber and trash cans waste combustion is lower than with wood pallets and higher than with cardboard boxes combustion. The impact of heatsink and lateral wind for TEGs system is also seen in each type of waste combustion.

It is noticed in operation conditions of TEGs without heatsink and with no lateral wind scenario have lower output power than with heatsink and with lateral wind. TEGs with heatsink and without lateral wind, and TEGs with no heatsink and with lateral wind scenarios have almost the similar results. Eventually, the impact of heatsink and lateral wind is noticed same in all types of waste combustion.

There is no doubt that, combustion of waste to produce power in this work provides an important solution to waste management. However, burning waste contributes to increasing of greenhouse gases level. Considering environmental-friendly and sustainable innovations as priority of the world we must apply some technologies for capturing carbon dioxide and particulate matter. It may affect the overall cost of power from this innovation. Secondly, the low energy conversion efficiency of TEGs enables us to produce low output power, thus may a drawback for this work. On the contrary, there are many works going on with better performance of TEGs and it is expected that TEGs with higher efficiency will be available soon in the market, which will of course make a better impetration on such kind of devices to make this work more worthwhile.

Finally, this work also highlights the significance of optimization techniques in enhancing the efficiency of thermal energy harvesting from waste burning. After a careful results analysis, TEGs operation conditions and waste types were identified, leading to increase the energy conversion rate and improve the overall performance of systems. This knowledge is crucial for future researchers aiming to design cost-effective and environmental-friendly type of waste for burning.

References

- [1]<https://www.sciencedirect.com/science/article/abs/pii/S2214785322049598>
- [2]<https://www.worldbank.org/en/topic/urbandevelopment/brief/solid-waste-management>
- [3] <https://www.ncbi.nlm.nih.gov/books/NBK233614/>
- [4]https://datatopics.worldbank.org/what-a-waste/trends_in_solid_waste_management.html
- [5]https://datatopics.worldbank.org/what-a-waste/trends_in_solid_waste_management.html
- [6]<https://landfillsolutions.eu/the-waste-to-energy-sector-in-spain-demands-measures-to-discourage-landfilling/>
- [7]<https://sdgs.un.org/goals>
- [8] <https://core.ac.uk/download/pdf/295537991.pdf>
- [9] <https://www.sciencedirect.com/science/article/pii/S2352484719306997>
- [10] <https://www.mdpi.com/1996-1073/13/14/3606>
- [11] <https://www.mdpi.com/2076-3417/13/4/2603>
- [12] <https://www.intechopen.com/chapters/65239>
- [13] <https://www.sciencedirect.com/science/article/pii/S2352484719306997>
- [14] <https://iopscience.iop.org/article/10.1149/2.F06083IF/pdf>
- [15] <https://journals.sagepub.com/doi/10.1177/0954407017733253>
- [16] <https://miscircuitos.com/how-to-characterise-a-thermoelectric/>
- [17] <https://www.elprocus.com/why-thermoelectric-generator-is-most-used-working-uses-and-benefits/#:~:text=Based%20on%20the%20TEG%20device,Solar%20source%20generators>
- [18] <https://www.intechopen.com/chapters/65239>
- [19] <https://www.mdpi.com/1996-1073/13/12/3185/htm>
- [20] <https://www.sciencedirect.com/science/article/pii/S0196890416311414>
- [21] http://cpb.iphy.ac.cn/article/2017/1907/cpb_26_10_104401.html
- [22] <https://www.worldbank.org/en/topic/urbandevelopment/brief/solid-waste-management>
- [23] https://datatopics.worldbank.org/what-a-waste/trends_in_solid_waste_management.html
- [24] <https://www.scielo.br/j/mr/a/6pQV5d6yY7dQfJj4pWNdyTv/>
- [25] <https://www.sciencedirect.com/science/article/pii/S266620272100001X>
- [26]<https://www.bioenergyconsult.com/effective-waste-management/#:~:text=The%20best%20way%20of%20dealing,landfill%20or%20dumpsite%20disposal%20technique.>
- [27] <https://www.ncbi.nlm.nih.gov/books/NBK233614/>
- [28] https://datatopics.worldbank.org/what-a-waste/trends_in_solid_waste_management.html
- [29]https://www.sciencedirect.com/science/article/pii/S1364032114002512?casa_token=SI57IZfRNgQAAAAA:QjgXTkSkDNY1sdfzjap16T0yTIOMs-9gWCPuxbjKtw9ckd0dklpgXH1w58feyv8GH407YZ0H#bib42
- [29]https://ec.europa.eu/eurostat/statistics-explained/index.php?title=Waste_statistics#Waste_treatment
- [30]<https://landfillsolutions.eu/the-waste-to-energy-sector-in-spain-demands-measures-to-discourage-landfilling/>
- [31]https://www.researchgate.net/publication/50273970_STUDY_ON_SOLID_WASTE_GENERATION_IN_KUANTAN_MALAYSIA_ITS_POTENTIAL_FOR_ENERGY_GENERATION
- [32]https://regions20.org/wp-content/uploads/2016/08/OPEN-BURNING-OF-WASTE-A-GLOBAL-HEALTH-DISASTER_R20-Research-Paper_Final_29.05.2017.pdf
- [33]https://ec.europa.eu/environment/archives/dioxin/pdf/stage1/incineration_industrial_wastes.pdf

- [34] <https://chemistry-europe.onlinelibrary.wiley.com/doi/full/10.1002/cssc.201600809>
- [35] <https://www.sciencedirect.com/science/article/pii/B9780750672948500208>
- [36] <https://www.nist.gov/el/fcd/multiple-item-transient-combustion-calorimetry>
- [37] https://www.fse-italia.eu/PDF/ManualiFDS/FDS_User_Guide.pdf
- [38] <https://www.tdx.cat/handle/10803/668544#page=1>
- [39] [xx] <https://ieeexplore.ieee.org/document/9258737>